Investigate the effects of molecular structure of lipidoids on self-assembly behavior

A thesis submitted by

Jun Wang

in partial fulfillment of the requirement

for the degree of

Master of Science

in

Biomedical Engineering

TUFTS UNIVERSITY

August 2015

Adviser: Professor Qiaobing Xu, Ph.D.

Abstract

Combinatorial library approach has been used to synthesize cationic lipid-based nanoparticles for developing new drug delivery system. Even though it is useful to identify the synthetic lipids with high efficiency, the fundamental mechanism of the structure-function correlation of the cationic lipids remains to be illustrated.

In this thesis, I primarily investigated the structure of the self-assembled cationic lipids using a combination of experimental and theoretic approaches, with an attempt to understand the mechanism of the varied delivery efficacy between lipids with similar structures. I used the fluorescence spectrometer measured the Critical Micelle Concentration (CMC) of the lipids from the library. The effects of the head group, disulfide bond and the length of the alkyl chains on the self-assembly behavior of the synthetic lipids were thoroughly investigated. Meanwhile, atomic force microscope (AFM) is used to study the morphology of the self-assembled lipid system. I also attempted to study the self-assembly of the lipids using molecular dynamic (MD) simulation. MD simulations showed that the synthetic lipids could aggregate in solution. The stability of the bilayer structure in simulation also indicated that the micelles or liposomes formed by lipidoids can maintain stability in aqueous solution.

The future work will contain several sections, including: i) to correlate the experimental study and MD simulation to illustrate the different self-assembly of various lipids with similar structures; ii) to generate an approach for rationale design the lipids with efficient delivery efficacy.

Acknowledgements

I would like to thank my research advisor Professor Xu for leading and guiding me during my master program, describing the meaning of scientific research, and providing advice for my research plan.

I would also like to thank Professor Atherton for teaching me how to conduct the molecular simulation. I would also like to thank my thesis committee member, Professor Cronin-Golomb, for his support and advice in my graduate study.

As for people in Professor Xu's lab, I would like to thank Dr. Wang for providing help and advice during my study and research; Pu Deng for teaching me how to prepare the lipidoid stock solutions; Jingqiong Xu for giving me advice about my project; Kyle Alberti for teaching me how to use necessary instruments for my project.

Finally, I would like to express my thanks to all the members in Professor Xu's lab. I appreciate their support and help in the lab.

Contents

List of Tables

List of Figures

Chapter 1 Introduction

1.1. Overview of Nanomedicine Field

Nanomedicine is the application of nanotechnology in clinical area such as the therapy[1], diagnosis, monitoring, and the control of the biological system. The targeted drug delivery system has especially become a popular research area in nanomedicine[2]. The size of these nanomaterials is very similar to that of biological molecules indicating that these nanomaterials can be applied as biological molecules in vitro or in vivo. Usually, in order to complete the specific function in vitro such as transporting pharmaceutical molecules, diagnosis of the human beings, the nanomaterials will combine with the specific molecules through different ways like conjugating the molecules, or surround the molecules, etc.

The nanomedicine has been widely studied and applied in many aspects of clinical research (See **Table 1**) such as the DNA manipulation, Drug delivery, diagnosis, biorobotics, etc[3].

Table 1 The application of nanomedicne[3]

A partial nanomedicine technologies taxonomy		
Raw nanomaterials	**Cell simulations and cell diagnostics**	**Biological research**
Nanoparticle coatings	Cell chips	Nanobiology
Nanocrystalline materials	Cell simulators	Nanoscience in life sciences
Nanostructured materials	**DNA manipulation, sequencing, diagnostics**	**Drug delivery**
Cyclic peptides	Genetic testing	Drug discovery

Dendrimers	DNA microarrays	Biopharmaceutics
Detoxification agents	Ultrafast DNA sequencing	Drug delivery
Fullerenes	DNA manipulation and control	Drug encapsulation
Functional drug carriers		Smart drugs
MRI scanning (nanoparticles)	**Tools and diagnostics**	
Nanobarcodes	Bacterial detection systems	**Molecular medicine**
Nanoemulsions	Biochips	Genetic therapy
Nanofibers	Biomolecular imaging	Pharmacogenomics
Nanoparticles	Biosensors and biodetection	
Nanoshells	Diagnostic and defense applications	**Artificial enzymes and enzyme control**
Carbon nanotubes	Endoscopic robots and microscopes	Enzyme manipulation and control
Noncarbon nanotubes	Fullerene-based sensors	
Quantum dots	Imaging (cellular, etc.)	**Nanotherapeutics**
	Lab on a chip	Antibacterial and antiviral nanoparticles
Artificial binding sites	Monitoring	Fullerene-based pharmaceuticals
Artificial antibodies	Nanosensors	Photodynamic therapy
Artificial ezymes	Point of care diagnostics	Radiopharmaceuticals
Artificial receptors	Protein microarrays	
Molecularly imprinted polymers	Scanning probe microscopy	**Synthetic biology and early nanodevices**
		Dynamic nanoplatform "nanosome"
Control of surfaces	**Intracellular devices**	Tecto-dendrimers
Artificial surfaces—adhesive	Intracellular assay	Artificial cells and liposomes
Artificial surfaces—nonadhesive	Intracellular biocomputers	Polymeric micelles and polymersomes
Artificial surfaces—regulated	Intracellular sensors/reporters	
Biocompatible surfaces	Implants inside cells	**Biotechnology and biorobotics**
Biofilm suppression		Biologic viral therapy
Engineered surfaces	**BioMEMS**	Virus-based hybrids
Pattern surfaces (contact guidance)	Implantable materials and devices	Stem cells and cloning
Thin-film coatings	Implanted bioMEMS, chips, and electrodes	Tissue engineering
	MEMS/Nanomaterials-based prosthetics	Artificial organs
	Sensory aids (artificial retina, etc.)	Nanobiotechnology

Nanopores	Microarrays	Biorobotics and biobots
Immunoisolation	Microcantilever-based sensors	
Molecular sieves and channels	Microfluidics	**Nanorobotics**
Nanofiltration membranes	Microneedles	DNA-based devices and nanorobots
Nanopores	Medical MEMS	Diamond-based nanorobots
Separations	MEMS surgical devices	Cell repair devices

1.2. Approach of Nanomedicine: Drug Delivery System (DDS)

1.2.1. Overview

As one of the most critical aspects in nanomedicine, the drug delivery system (DDS) has multiple advantages compared to conventional therapies such as decreasing the side effects when curing cancers[4].

Since the drug delivery system (DDS) is a method of transporting the pharmaceutical molecules through different membranes like the blood-brain barrier, cell membrane to achieve the therapeutic effects, it is more convenient than conventional drug therapies. It may involve the site-targeting within the patient's body or the systemic pharmacokinetics. Since this method can improve the drug release system and the transportation system, the pharmaceutical compounds can be better distributed and last longer in the human body.

Targeted drug delivery is an improved approach of drug delivery which can transport the pharmaceutical to the targeted site within human body and release the drug under control. Through targeted drug delivery, the dose of the drug can be reduced and the therapy can be more effective and specific, as in some cases targeted drug delivery is also known as the smart drug delivery.

1.2.2. Delivery Vehicles

According to the biomaterials applied in DDS, drug delivery system can be categorized into several classes, such as the lipid-based drug delivery, polymer-based drug delivery, etc.

1.2.2.1. Lipid

With the development of pharmaceutical research, more drugs have shown poor solubility in water, which has restricted the clinical application. In order to improve the solubility of the drugs, especially for oral drugs, the lipid-based drug delivery system (LBDDS) was developed[5, 6]. For example, Prabhu et al found that with the combination of the lipid-based vehicle, polyethylene glycol (PEG 4600) and 1,2-dimyristoyl-sn-glycero-3-phosphatidylcholine (DMPC) phospholipid, the effects of the piroxicam (PXCM) that had poor solubility in water could be improved significantly[7].

1.2.2.2. Polymer

Another widely used materials for drug delivery is polymer. Compared to other methods, the advantages of polymeric micelles can be summarized as several different aspects. First, through supramolecular assembly, they can form the environmentally-separated microcontainer of the drugs. Second, the stability of the delivery system is controllable. Third, the delivery system can conjugate the anchoring moiety on its surface[8]. According to the specific techniques used in the polymeric-based drug delivery system, they can be categorized as several different types: diffusion-controlled system, solvent-activated system, chemically controlled (bioreducible) system, and the responsive system[9].

1.2.2.3. Inorganic nanoparticles

Inorganic nanoparticles are potential vehicles considering their physicochemical properties. Since the size of the inorganic materials is very small, the ratio of surface area to volume is very high. As a result, their physical properties, such as optical and magnetic properties, will be very different and their affinity to targeted molecules will be improved with the ligands[10]. For example, in **Figure 1**, Liong et al incorporated the magnetic iron oxide nanocrystals in the silica nanoparticles. Then the anticancer drugs were added into the pores of the nanoparticles. The surface of the nanoparticles are coated with phosphonate and targeting ligands. Through such modification, the nanoparticles have multiple functions during the cancer therapy. They can be used to release the anticancer

drugs at the specific sites according to the recognition capability of the ligands and the iron oxide magnetic nanocrystals play the critical role in MR imaging[11].

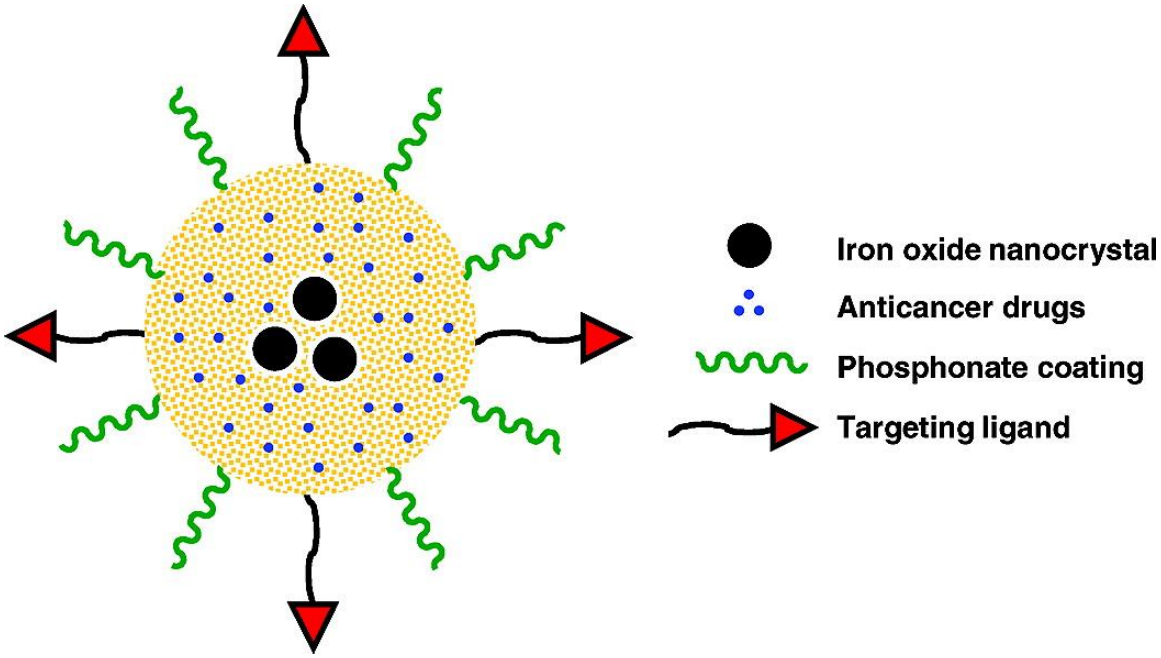

Figure 1 The composition of the multifunctional nanoparticles[11].
The iron oxide nanocrystal is incorporated in the silica nanoparticles which is yellow point in the figure. The iron oxide nanocrystal is magnetic and can be utilized in MR imaging. Then the anticancer drugs are also distributed into pores of the nanoparticles. The phosphonate coating can improve the stability of the dispersion of the nanoparticles in solution. The targeting ligand is used for specific recognition for targeted drug delivery.

1.3. Combinatorial Library of Lipidoids

1.3.1. Previous Research

Lipidoids are a class of lipid-like molecules which can be used as the delivery vehicles for genes and proteins. Akin et al developed the chemical methods to realize the rapid synthesis of a large library of different types of lipidoids[12]. They utilized the Michael addition to conjugate the aliphatic amines and different types of lipophilic chains to form the double-chain lipid-like molecules[12, 13, 14]. These lipidoids have been proved to be able to achieve the high level of silencing of the specific gene expression with the small interfering RNA (siRNA)[12, 13]. Sun et al indicated that some of them had better transfection efficiency of DNA delivery than that of Lipofectamine 2000, which is a widely used standard for the in vitro gene delivery[15].

Initialized through conjugating the amine groups with three types of alkyl chains (acrylamide, acrylate, and epoxide) (See **Figure 2**). Sun et al synthesized a refined library of lipidoids which are purified for DNA delivery[15].

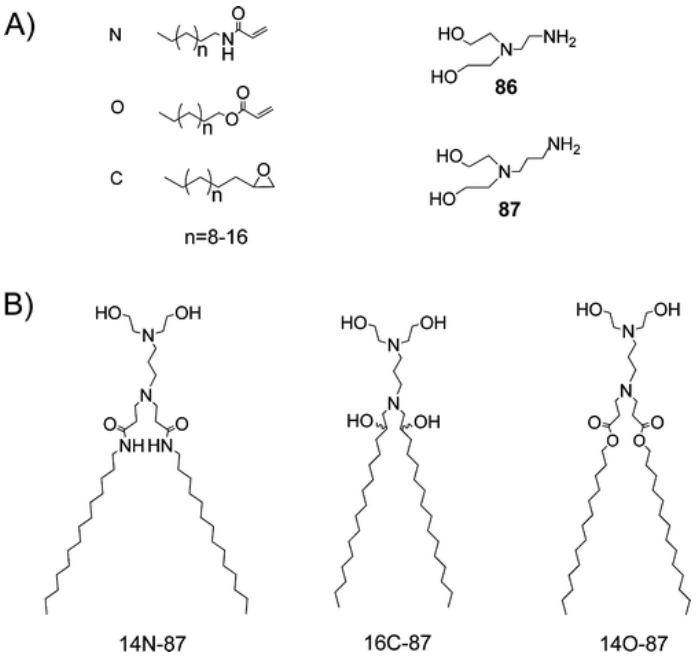

Figure 2 The scheme of the combinatorial library of the lipidoids for DNA delivery[15]. There are two different amine groups and three different alkyl chains for assembly.

Inspired by the initial research of Sun et al, Wang et al discovered the lipidoids which was modified from the combinatorial library of lipidoids from Sun et al. He synthesized the lipidoids with unsaturated alkyl chains at first and proved these lipidoids' capability of gene delivery[16] (See **Figure 3**). Then he and his colleagues synthesized the lipidoids with disulfide bond and also indicated that these bioreducible lipidoids could complete the gene transfection[14] (See **Figure 4**).

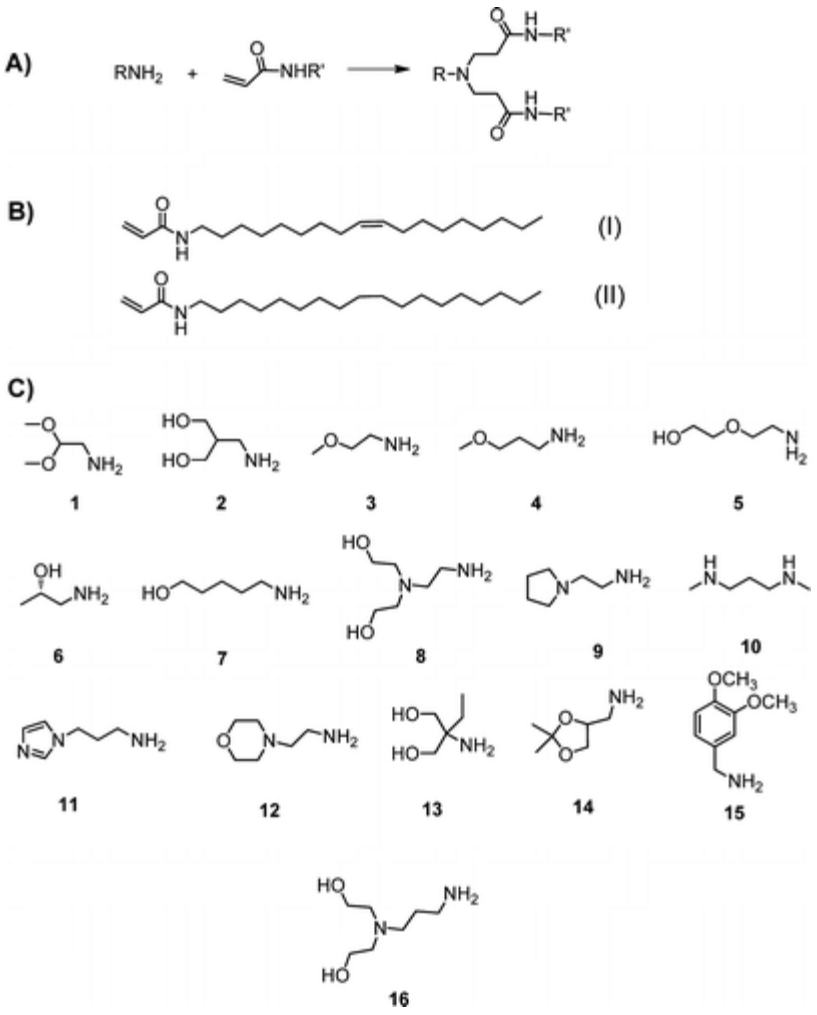

Figure 3 The combinatorial library of unsaturated lipidoids[16].
There are 16 kinds of different amine groups and 2 different types of alkyl chains (one is saturated and the other is unsaturated.)

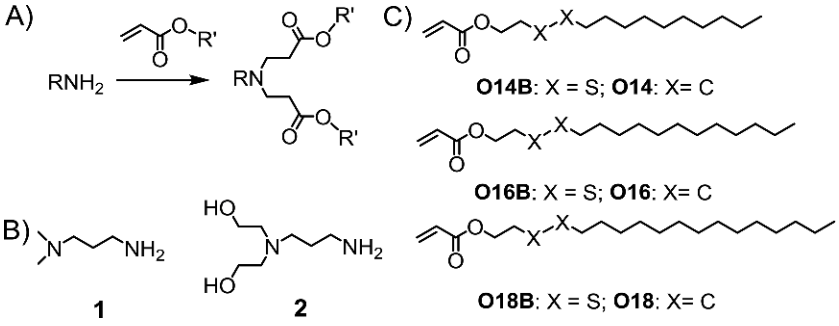

Figure 4 The combinatorial library of bioreducible lipidoids[14].

There are two different types of amine groups and six different types of alkyl chains (three chains have disulfide bonds and the others have no disulfide bond). These lipidoids are the samples we are going to measure in the thesis.

1.3.2. Application

In order to test the delivery effects of these lipidoids synthesized in Dr. Xu's lab, Sun et al and Ming et al conducted the gene delivery and protein delivery by these lipidoids and the results indicated that these lipidoids could show good property for transporting the genes and proteins into cells[15, 14, 16, 17, 18].

1.3.2.1. Nucleic acid delivery

As previous description, since these lipidoids could be divided into three categories according to the alkyl chains in the lipidoids: saturated lipidoids, unsaturated lipidoids, and bioreducible lipidoids. The effects of the nucleic acid delivery of these lipidoids were compared from these three different aspects.

At first, the transfection efficiency of DNA delivery by the lipidoids in the initial combinatorial library varies according to different types of amines or alkyl chains. For example, according to the previous research (See **Figure 5**), the lipidoid named 14N-87 which is composed of the "87" head group and the alkyl-acrylamide has a much higher transfection efficiency than that of the Lipofectamine2000, while the lipidoid named16O-

86 which is composed of the "86" head group and the alkyl-acrylate has nearly no transfection effects comparing to Lipofectamine2000[15].

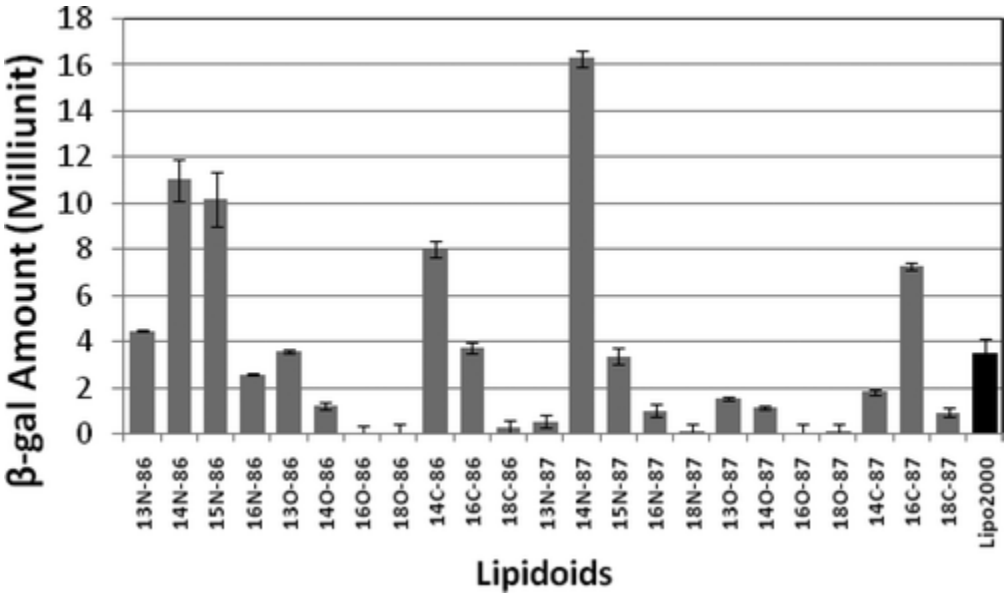

Figure 5 The β-gal expression by DNA delivery through different lipidoids[15]. Through delivering plasmid DNA encoding β-gal into cells, the delivery efficiency of lipidoids and Lipofectamine 2000 were tested. The result indicated that some of the lipidoids have better capability for drug delivery comparing to Lipofectamine 2000, while some don't.

Then considering the effects of the saturation of the alkyl chains on the delivery efficiency, Wang et al synthesized the unsaturated lipidoids (See **Figure 3**). The GFP expression by DNA delivery or mRNA delivery through these lipidoids were also tested (See **Figure 6**). From this figure, it was visible that some of the lipidoids had very strong capability for delivering DNA or mRNA into cells. In fact, some of the lipidoids even had better delivery efficiency than Lipofectamine 2000. It was also clear that the unsaturated lipidoids have much better delivery capability than that of the saturated lipidoids[16].

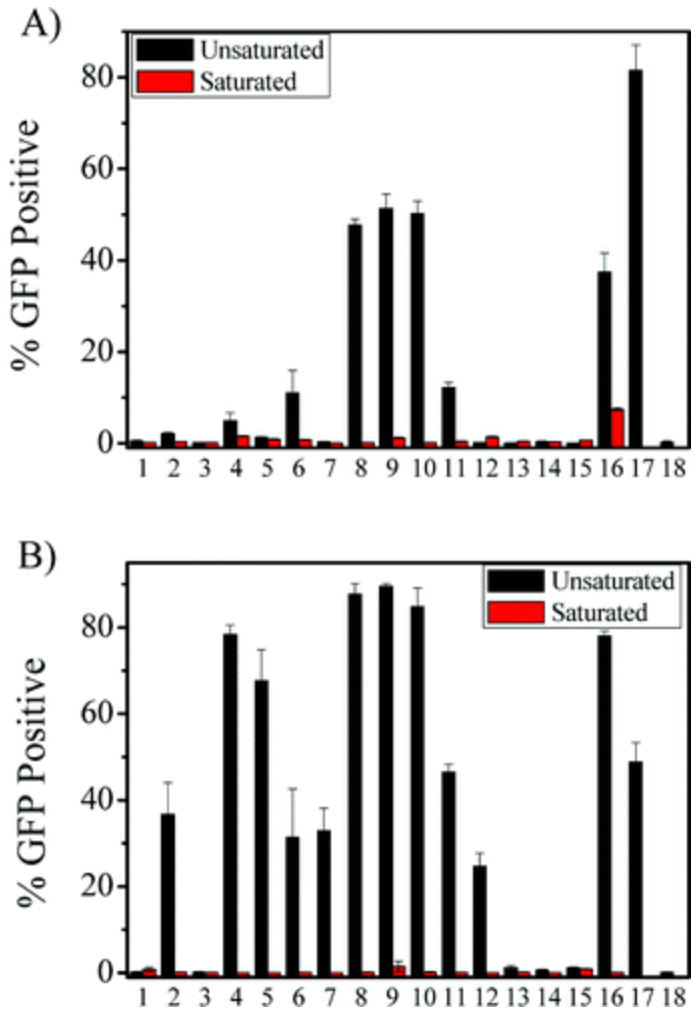

Figure 6 The efficiency of DNA and mRNA by different lipidoids[16].
(A) The GFP positive with DNA delivery by lipidoids (B) the GFP positive with mRNA delivery by lipidoids. 1-16: DNA or mRNA delivery with the corresponding lipidoids; 17: DNA or mRNA delivery with Lipofectamine 2000; 18: DNA or mRNA delivery without carrier

Wang et al also measured the efficiency of the bioreducible lipidoids for delivering small interfering RNA (siRNA) into cells (See **Figure 7**). They synthesized the bioreducible lipidoids by using disulfide bond to replace two carbon atoms on the alkyl chains (See

Figure 4). From the GFP expression, it was visible that the bioreducible lipidoids with the siRNA could suppress the GFP expression in cells significantly, which indicated that the disulfide bond in the bioreducible lipidoids could improve the efficiency of siRNA delivery[14].

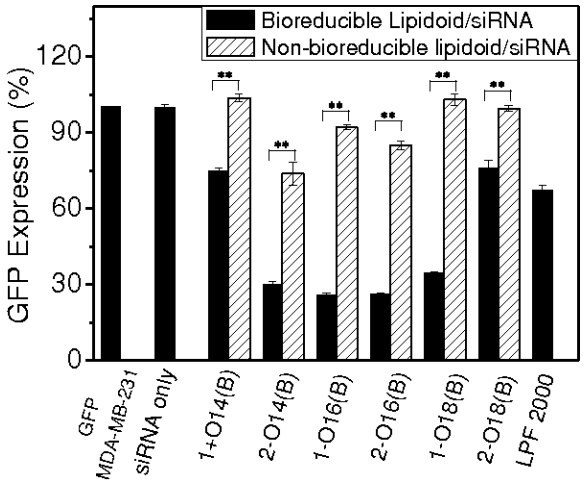

Figure 7 The GFP expression of GFP-MDA-MB-231 cells treated with different methods[14].

1.3.2.2. Protein delivery

To investigate the efficiency of protein delivery by the lipidoids, Wang et al synthesized the lipidoids through conjugation of different amine groups with 1,2-epoxyhexadecane[17] (See **Figure 8**). In order to determine the delivery efficiency, two different cytotoxic proteins (RNase A and saporin) were utilized. According to the cell viability, it was visible that the existence of the lipidoids with not proteins didn't affect the cell viability, indicating that the lipidoids had no cytotoxic properties themselves. On the other couldn't hand, the naked proteins like RNase A and saporin had nearly no effects on cell viability

as well, which meant that these proteins enter into cells by themselves. However, after conjugating with the lipidoids, some of the combinations show strong cytotoxic properties. For example, the combination of EC16-1 and saporin and saporin-Aco (See **Figure 9**) could decrease the cell viability significantly. These results indicate that the lipidoids show good efficiency when transporting proteins into cells.

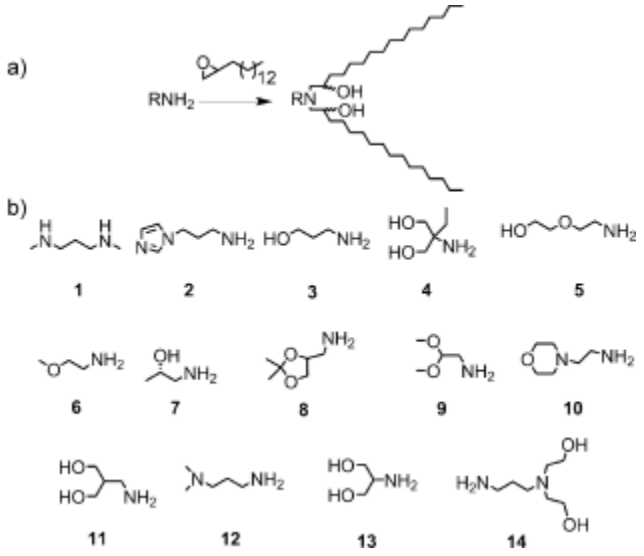

Figure 8 The formulation of the lipidoids for protein delivery[17]

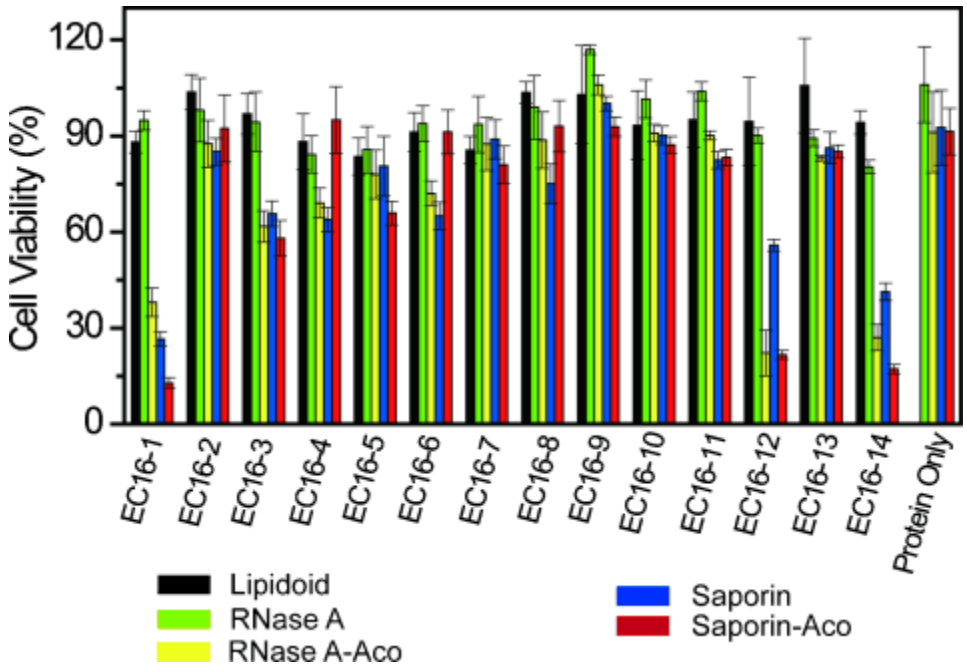

Figure 9 The cell viability after cytotoxic protein delivery by lipidoids[17].
The cell line is B16F10 cell line. Black: 4 μg/mL; Green: 3.3 μg/mL; Yellow: 3.3 μg/mL; Blue: 0.17 μg/mL; Red: 0.17 μg/mL.

Chapter 2 Overall Object

Since many researches have indicated that lipidoids had good efficiency for gene delivery and protein delivery, it is necessary to expand the combinatorial library of the synthesized lipidoids. However, according to the previous description of the application in gene delivery and protein delivery, even though most of the lipidoids show good capability for drug delivery, their efficiency varies significantly. Understanding the reason why these lipidoids have different efficiency in gene delivery and protein delivery can provide theoretical support for expanding our combinatorial library in the future.

According to the study on the unsaturated lipidoids and bioreducible lipidoids, the difference in the alkyl chain may affect the delivery efficiency significantly. These conclusions led us believe that the difference in structure may cause the difference in function for drug delivery, so we combined the experimental method with molecular simulation to investigate the effects of the structures of the lipidoids on the self-assembly behavior in aqueous solution to understand the reason of the difference in delivery efficiency from a physical perspective.

2.1. Experimental Study

In experimental study, we studied the self-assembly behavior and the morphology of the micelles of the lipidoids.

Critical Micelle Concentration (CMC) is one of the critical parameter to indicate the tendency of self-assembly in aqueous solution and it was measured by the 1:3 ratio method with the fluorescence spectrophotometer. The morphology of the micelles was observed through AFM.

2.2. Simulation Study

In simulation study, the self-assembly behavior of the lipidoids was investigated by two different types of simulation. The first one was the aggregation simulation of multiple molecules distributed at random and the second one was the simulation of bilayer structure formed by multiple lipidoids.

Chapter 3 Study of self-assembly of lipidoids by experiment

3.1. Introduction

3.1.1. Measure Critical Micelle Concentration (CMC) of lipidoids by using fluorescence spectrophotometer

3.1.1.1. Self-assembly behavior of lipidoids in aqueous solution

Surfactants are composed of two different components. The first component is the head group which is hydrophilic while the other component is the hydrophobic chain (See **Figure 10**). This characteristic of surfactants determines its unique behavior in solution. For example, if the water solution of the surfactant is in contact with oil, the surfactants usually tend to distribute at the interface between the oil and water, because the hydrophilic component of surfactant tends to contact the water molecules while the hydrophobic component of the surfactant tends to contact the oil molecules (See **Figure 11**). This is the reason why surfactants have tendency of self-assembly in water. Through forming micelles, or bilayer structure, the hydrophobic component of the surfactants can stay in the nonpolar environment and the hydrophilic component of the surfactants can stay in contact with the water molecules which is in the polar environment.

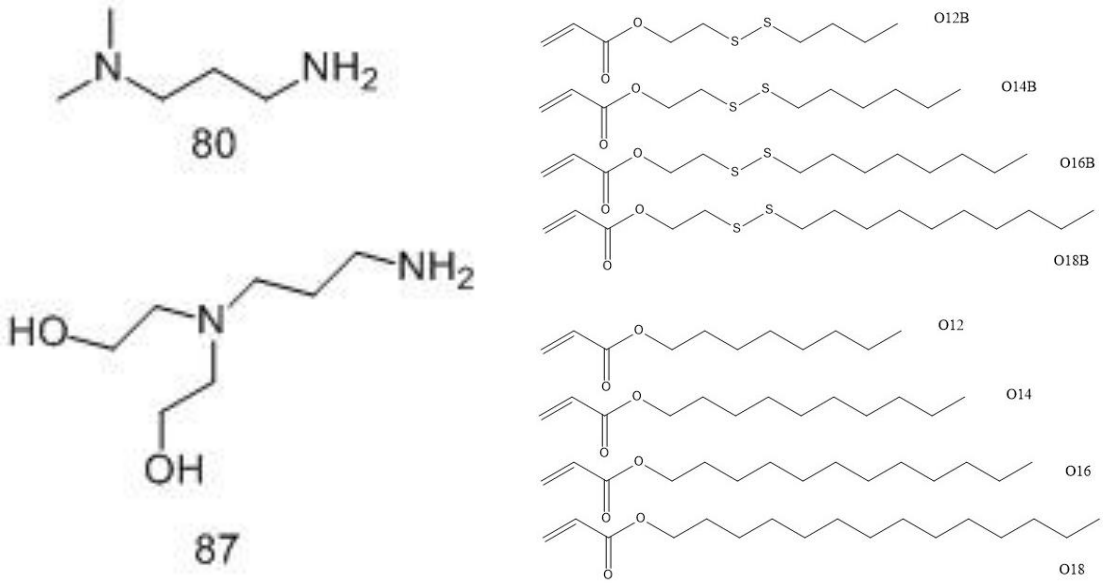

(a) (b)

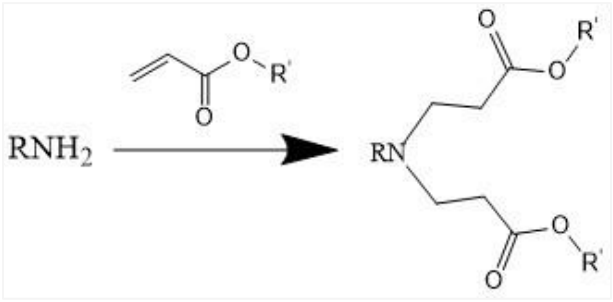

(c)

Figure 10 The molecular structure of the lipidoid molecules.
(a) The hydrophobic group in the lipidoid molecules. (b) The hydrophilic group in the lipidoid molecules. (c) The combination of the hydrophobic component and the hydrophilic component.

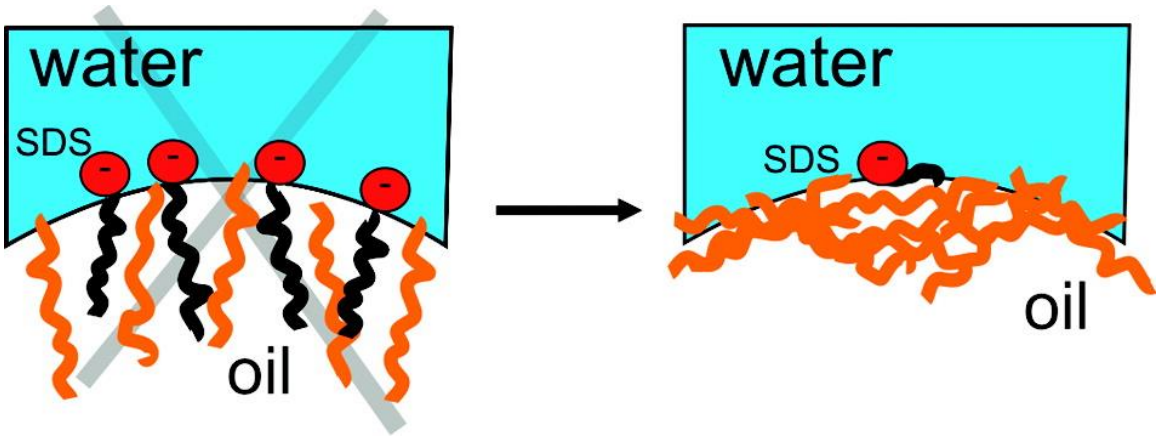

Figure 11 The distribution of the surfactant molecules (SDS) at the interface between the oil and water[19].

Considering the structure of lipidoids in the previous description, it is easy to conclude that these lipidoids are also surfactants. The amine groups are the hydrophilic groups while the alkyl chains form the hydrophobic groups in the lipidoid molecules (See **Figure 10**). Thus, these lipidoids will also show self-assembly behavior. In fact, the TEM evidence have proved that these lipidoids can form bilayer structure or micelle structure in aqueous solution (See **Figure 12**)[15]. Thus, investigation of the self-assembly behavior will be a feasible approach to study the effects of the structure on the physical property of the lipidoids in solution.

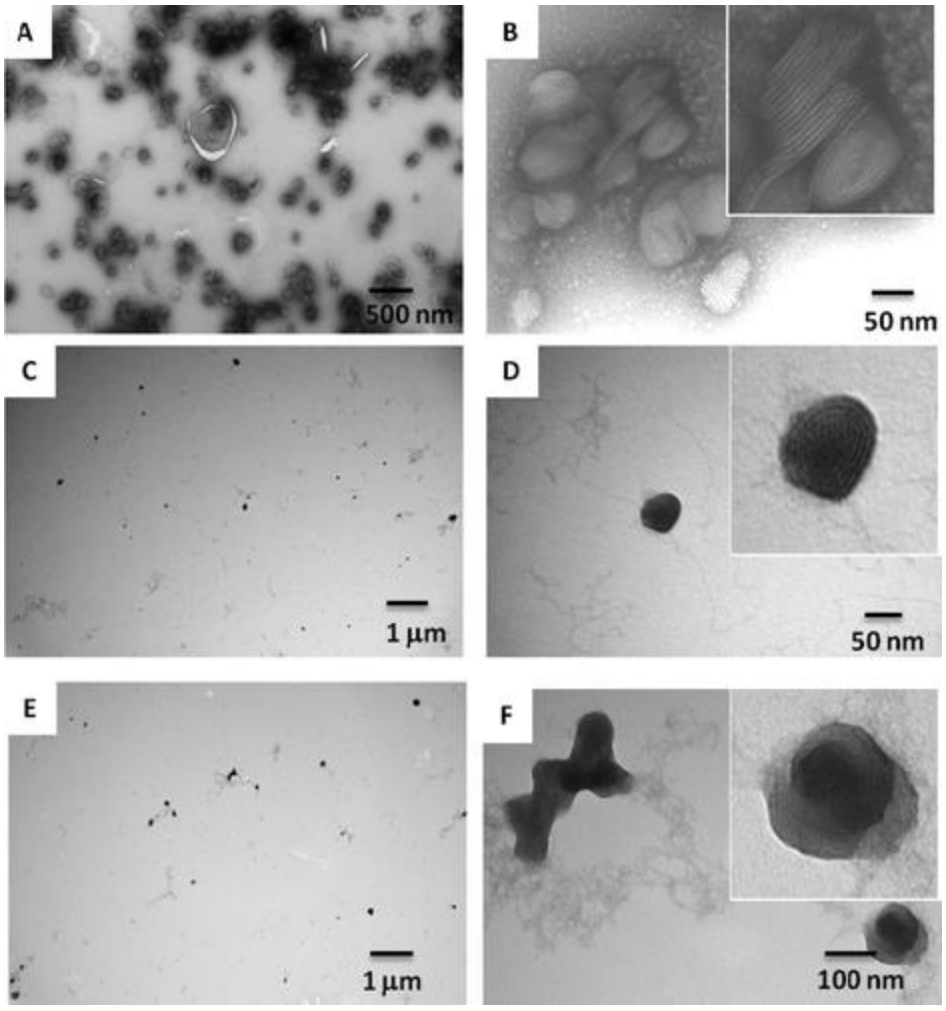

Figure 12 The negative staining TEM images of self-assembly behavior of different lipidoids nanoparticles[15].
A and B: 14N-87/DNA complex; C and D: 16C-87/DNA complexes; E and F: 14O-87/DNA complexes

3.1.1.2. Critical Micelle Concentration (CMC)

CMC (Critical Micelle Concentration) is defined as a specific concentration of the detergent in the solution[24]. When the concentration of the detergent is lower than CMC, they won't form micelle in the solution. On the other hand, when their concentration is larger than CMC, they will form micelles in the solution.

As one of the critical delivery vehicles in the drug delivery system (DDS), it is necessary to make sure that the surfactants can form micelles when preparing the pharmaceutical device. Thus, through measuring the CMC value of the surfactants, it provides a convincing method to determine the concentration of surfactants in the medium for transportation. On the other hand, the CMC value itself can also profile the tendency of self-aggregation of the surfactants significantly, through comparing the difference of the CMC values, it is feasible to indicate whether the lipidoids can form micelles very easily in the solution.

3.1.1.3. Methods to measure CMC value

3.1.1.3.1. Conventional methods

There are many different ways to measure CMC, such as UV-Absorption Spectroscopy Method, Electrical Conductivity Method, Surface Tension Method, Light Scattering Method, etc[23].

However, these conventional methods are restricted by various disadvantages. For example, light scattering method is not sensitive if the CMC of the surfactant is very low and it can only provide the CMC value in a very large range[20, 21]. Comparing to these

conventional method, the fluorescent method by pyrene is much more sensitive to the subtle change of the CMC value even when it is very low[21].

3.1.1.3.2. 1:3 ratio method

Pyrene has poor solubility in water, thus it will be distributed in the water solution as crystal and exhibits the fine structure when the emission wavelength is within the range of 370-400 nm[22] (See **Figure 15**). The intensity of the peak in the spectrum is dependent on the polarity of the environment. For example, in the presence of polar solvents like water, it is observed the enhancement of the intensity of the 0-0 band with the decrease of the other peaks' intensity. In fact, the dipole moment and the dielectric constant of the solvent are both important to Pyrene[23]. Among these changes of the spectrum of the pyrene, the variation of the ratio of the first vibronic peak to the third vibronic peak is the greatest, thus, this ratio (or called 1:3 ratio) has become a widely used approach to determine the CMC value of the surfactants. When the concentration of the surfactants in the solution is below the CMC value, they will not form micelle so that the pyrene crystal is distributed in the solution and surrounded by the water molecules which have high polarity. The 1:3 ratio is high at this moment. When the concentration of the surfactant is above the CMC value, pyrene crystal will be surrounded by the formed micelles in the solution which has lower polarity comparing to the water molecules. Then, the 1:3 ratio will decrease at this moment (See **Figure 13**). This changing pattern of the 1:3 ratio with the increase of the concentration of the surfactants in the solution can be described by the Sigmoidal Equation[24] (See **Figure 14**):

$$y = \frac{A_1 - A_2}{1 + e^{\frac{(x - x_0)}{\Delta x}}} + A_2 \quad (1)$$

In this equation, the variable y represents the 1:3 ratio of the pyrene. The variables A_1 and A_2 represent the upper and lower constant in the 1:3 ratio curve. The variable x represents the concentration of the surfactants and the variable x_0 represents the center of the sigmoid. The variable Δx represents the difference between the concentrations of the samples.

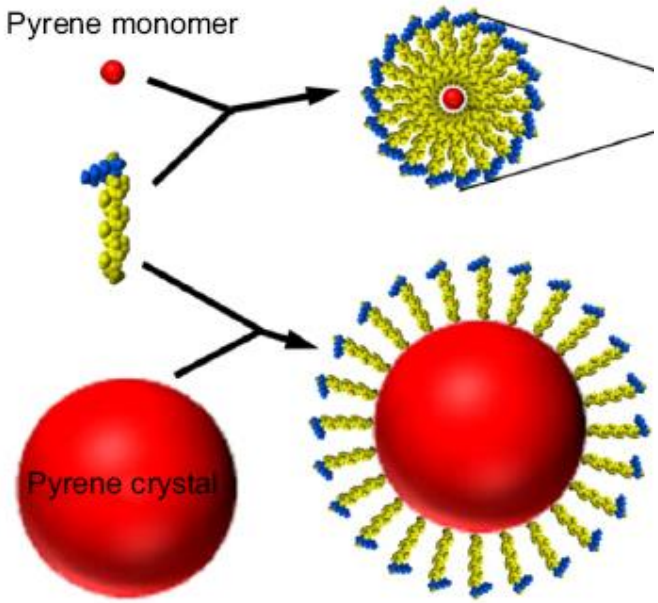

Figure 13 The molecular structure of the combination of the pyrene crystal and the micelles distributed in the solution[25]

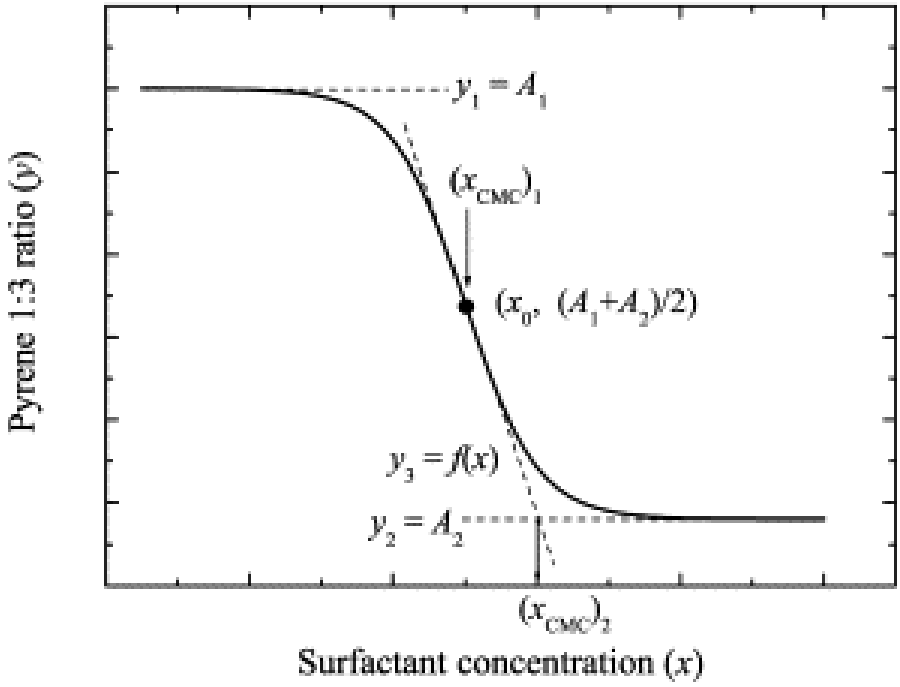

Figure 14 The fitting curve and the corresponding parameters in the sigmoidal equation[24]

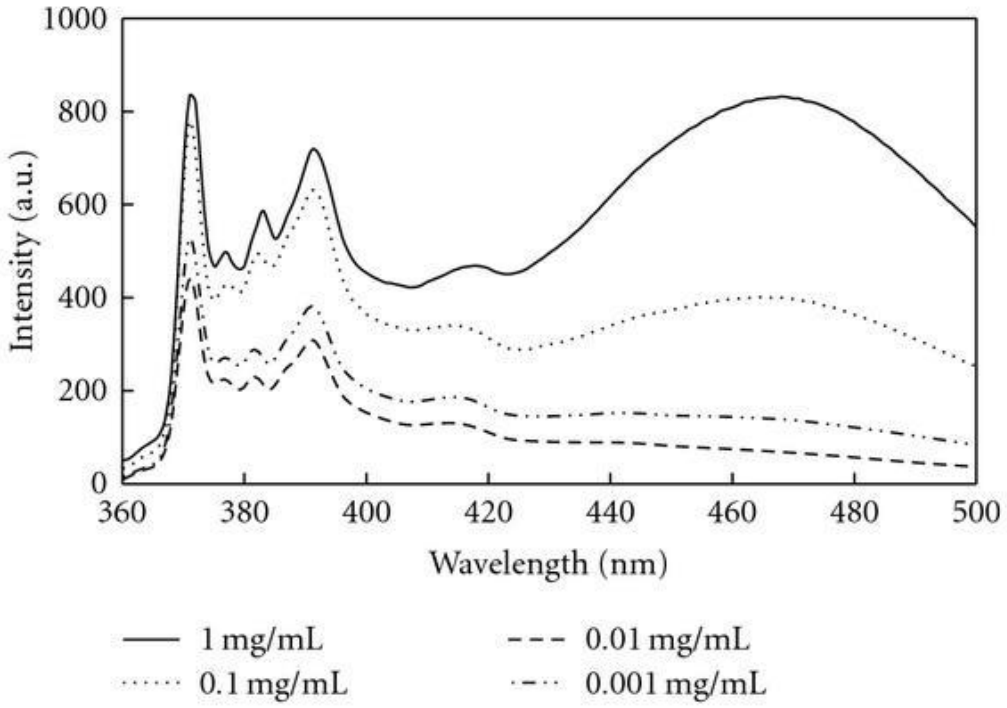

Figure 15 The emission spectra of pyrene from 360 nm to 500 nm[26].

3.1.2. Characterize the morphology of micelles of lipidoids by using Atomic Forces Microscopy (AFM)

Atomic Force Microscopy (AFM) is a scanning probe microscopy with a high resolution (lateral resolution is around 30 Å and the vertical resolution is less than 1 Å)[28]. It can be used to distinguish the morphology of the sample within nanometers. The Scanning Tunneling Microscope (STM) was invented in IBM by Gerd Binning and Heinrich Rohrer, who earned the Nobel Prize for Physics because of this invention in 1986[27]. In order to overcome of the disadvantages of STM, Bining invented the Atomic Force

Microscopy in 1986 and made the first experimental implementation in 1986 as well with his colleagues, Quate and Gerber[28]. Finally, in 1989, they introduced the first commercially available AFM instrument.

AFM instrument is consisted of several critical components: cantilever, sharp tip, detector, xyz-drive, controllers and plotter, etc[29]. A cantilever is usually in the scale of micrometers and the sharp tip exists at the end of the cantilever. The radius of the tip is usually from several nanometers to a few tens of nanometers. During the scanning of the surface of the sample under different modes, the cantilever will be deflected because of the interaction with the surface of the sample. This deflection of the cantilever will cause a specific changing pattern of the laser beam on the cantilever. Through receiving the signal of the laser reflected by the cantilever, the morphological pattern such as the height of the samples can be collected.

Since there are three different modes in AFM[30], it is necessary to select the proper mode for observing the morphology of micelles through AFM.

3.1.2.1. Contact Mode

There are two ways in the contact mode to generate the signal which can profile the morphology of the surface of the samples. The first way is the deflection of the cantilever caused by interaction with the samples such as the van der Waals' force, capillary force,

electrostatic forces, etc. Another way is to receive the feedback signal which is required to keep the position of the cantilever stable. Since the tips are closed to the surface of the sample, contact mode may cause the damage on the samples. As a result, it is not sufficient to utilize the contact mode for some of the samples such as the soft samples.

3.1.2.2. Noncontact Mode

Compared to the contact mode, the non-contact mode can overcome the disadvantage of the contact mode. For non-contact mode, tips will not touch the samples, leading to no damage to the samples. Instead, the cantilever will be oscillated at the frequency which is slightly above the resonant frequency. Since the interaction of the tip and the samples like the van der Waals' force will affect the frequency and the amplitude, it is feasible to know the change of the distance between the tip and the surface of the sample through analyzing the changing pattern of the frequency or the amplitude of the cantilever.

3.1.2.3. Tapping Mode

Since samples may have a liquid meniscus layer on the surface, tapping mode was developed in order to avoid the tips sticking to the surface [31]. In tapping mode, the cantilever will move up and down at the frequency which is closer to the resonant frequency and the amplitude will be around 100-200 nanometers. Since when the tip on the cantilever is getting closer to the surface of the sample, the interaction between the tip

and the sample like the van der Waals' force, electrostatic force, etc. will make the amplitude smaller. On the other hand, the electronic servo will keep the amplitude stable through adjusting the distance between the tip and the sample. Then, the pattern of the surface of the sample will be collected[32]. Since the tapping mode will decrease the damage to the sample and the tip, all the micelle samples prepared here will be measured by this mode.

3.2. Materials and Methods

3.2.1. Material

3.2.1.1. Chemicals

Pyrene was purchased from Sigma-Aldrich (St. Louis, MO) and used for the preparation of the pyrene stock solution directly. The sodium acetate buffer solution (3M) was purchased from Sigma-Aldrich (St. Louis, MO) and then diluted with ultra-pure water until the concentration was 25mM. The ethanol was purchased from Sigma-Aldrich (St. Louis, MO) and used for the preparation of the solution directly. All the lipidoids were provided by Dr. Ming in Dr. Xu's lab. For convenience of the description of the lipidoids, all lipidoids will be named after its head group and the alkyl chain (See **Figure 10**). In **Figure 10**, the head groups include the "80" head group and the "87" head group. The alkyl chain is named after the acrylate number of the chain and whether the chain contains a disulfide bond. For example, the lipidoid has an "80" head group, its acrylate

number of alkyl chain is 16 and it has disulfide bond, so then this lipidoid is called 80O16B.

3.2.1.2. The instrument and its configuration

3.2.1.2.1. 1:3 ratio method for measuring CMC

The Fluorescence Spectrophotometer (F-4500, HITACH, Japan) was used to measure the emission spectra and the excitation spectra. All the measurements were conducted at room temperature with a 5 mm path length quartz cuvette.

The configuration for the measurement of the emission spectra is listed below.

Table 2 The configuration setting of the fluorimeter

Excitation wavelength	335 nm
Emission wavelength	360 nm ~ 400 nm
Excitation slit	2.5 nm
Emission slit	2.5 nm
Scanning speed	60 nm/min

3.2.1.2.2. Using AFM to observe the morphology of the micelles

The mode of Atom Force Microscope (AFM) (Dimension^{TM} 3100, Veeco, Lowell, MA) for the measurement is tapping mode and other configurations for the tapping mode.

3.2.2. 1:3 ratio method to measure the CMC value

3.2.2.1. Preparation of the lipidoid stock solution

The pure lipidoids were stocked in the fridge at 4℃. Before the experiment, the lipidoids were taken out from the fridge and were solvated in determined amount of the 25 mM sodium acetate buffer (diluted with ultra-pure water from the 3 mM sodium acetate buffer). The final concentration of the lipidoid stock solution should be 1 mg/mL before the experiment.

3.2.2.2. Preparation of the pyrene stock solution

Considering the low solubility of the pyrene in the water, the amount of the pure ethanol was determined beforehand. The final concentration of the pyrene in the pure ethanol should be 4 mM and then stocked in the fridge at 4℃.

To avoid the precipitation of the pyrene in the water, which may cause error in the fluorescent excitation, the pyrene stock solution was diluted only with ethanol and distilled water before the measurement. For the dilution of the pyrene, the pyrene was diluted with a determined amount of pure ethanol so that the final concentration of the pyrene in the ethanol solution should be 400 μM. Then, the diluted pyrene stock solution

was diluted with distilled water to make the final concentration of the ethanol to be 20%wt and the concentration of the pyrene in this solution should be 80 μM.

3.2.2.3. Preparation of the sample solution for the fluorescence measurement

Since ethanol will affect the polar environment of the solution and the self-assembly of the lipidoid, it is necessary to make sure that the concentration of the ethanol should be low enough for it to be negligible during the experiment. Here, the concentration of the ethanol in the sample solution was diluted to 0.5%wt which is considered to be small enough to have no effects on the measurement[33] . Thus the concentration of the pyrene in the sample solution should be 2 μM.

The procedure to prepare the sample solution was: First, add the determined amount of sodium acetate buffer (25 mM) into the tube. Then, add 50 μL of pyrene solution (80μM) into the acetate buffer solution. Finally, add the determined amount of the lipidoid stock solutions into mixture to make the final volume of the sample solution to be 2 mL.

After preparation of the mixture solution, in order to make sure that the pyrene molecules and the lipidoid molecules were all well-distributed in the sample solution, the mixture was sonicated for 5 minutes before the measurement. After the sonication, the sample

solution was transferred into the quartz cuvette and the sample was measured with the fluorescence spectrophotometer.

3.2.3. Characterize the morphology of micelles by AFM

3.2.3.1. Preparation of the sample for AFM

The sample solution of the lipidoids was prepared at the specific concentration (1 mg/mL). Since the goal of utilizing AFM for the measurement was to observe the morphology of the micelle formed by the lipidoid molecules, the concentration of the lipidoids in the sample solution should be larger than the CMC value.

The tape was used to clean the surface of the mica and then one to two drops of the sample solution were dropped on the mica, which was fixed on the glass slide. The sample was left out for approximately two hours and the sample solution on the mica should have evaporated. The mica was washed with the distilled water gently and removed the remaining water on the mica with tissue. Then the sample for AFM measurement was prepared.

3.2.3.2. Steps for initializing the AFM instrument for tapping mode

1) Click the software named Nanoscope and the AFM instrument will be turned on automatically.
2) Mount the support with the cantilever and the tip onto the AFM instrument.
3) Adjust the position of the camera so that the tip is in the middle of the camera.
4) Adjust the orientation of the laser to get the diffraction of the laser at the tip of the cantilever.
5) Move the position of the red dot to the middle of the cross in the meter window.
6) Place the sample on the stage. Then, locate the tip and the surface of the instrument and then complete the cantilever autotune.
7) After the cantilever autotune, check the configuration in the parameter list. Set scanning mode as tapping mode. Then adjust other parameters according to the situation.

3.3. Results and Discussion

3.3.1. 1:3 ratio method to measure CMC of lipidoids

3.3.1.1. Validate the 1:3 ratio method by measuring SDS

Though the 1:3 ratio method to measure CMC is relatively accurate and sensitive according to the previous research[21], it is still necessary to set up an accurate experiment protocol for the measurement of CMC and to prove its accuracy in our lab. Thus, the

emission spectrum and the excitation spectrum of the sodium dodecyl sulfate was measured at first.

3.3.1.1.1. The emission spectra and the excitation spectra

(a)

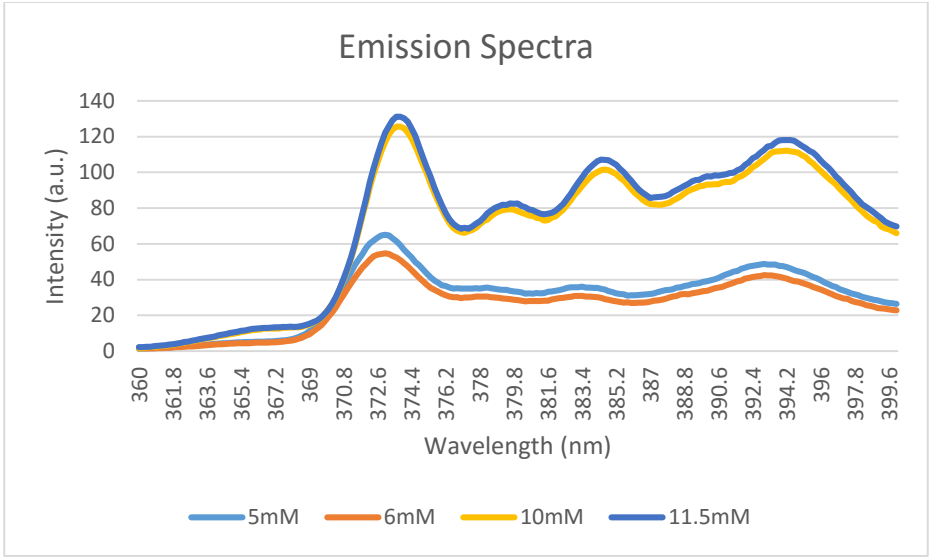

(b)

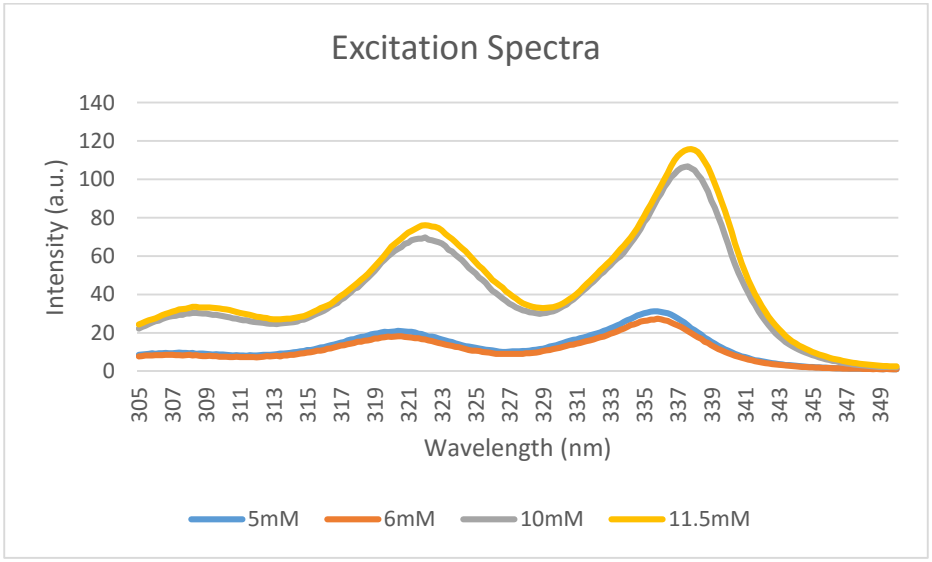

Figure 16 The emission spectrum and the excitation spectrum of SDS at different concentration.
(a) emission spectra (b) excitation spectra

According to the reference[26], there are two characteristics for the emission spectra and the excitation spectra. First, there are four peaks in the region where the emission wavelength is from 360 nm to 400 nm (See **Figure 15**). This conclusion is the same as the emission spectra of SDS in **Figure 16**. Second, with the increase of the concentration of the surfactant in the solution, the intensity of the spectrum should increase, which is also the same according to the emission spectrum and the excitation spectrum. These results indicate that the fluorescent method for measuring the emission spectra of pyrene in SDS solution is feasible.

3.3.1.1.2. The CMC value of SDS

According to the previous description of the 1:3 ratio methods, the 1:3 ratio at all different concentration of the surfactants should meet the Sigmoidal Equation, so we could utilize Mathematica to find the fitting result of the equation with the 1:3 ratio at different concentration. The fitting result is below:

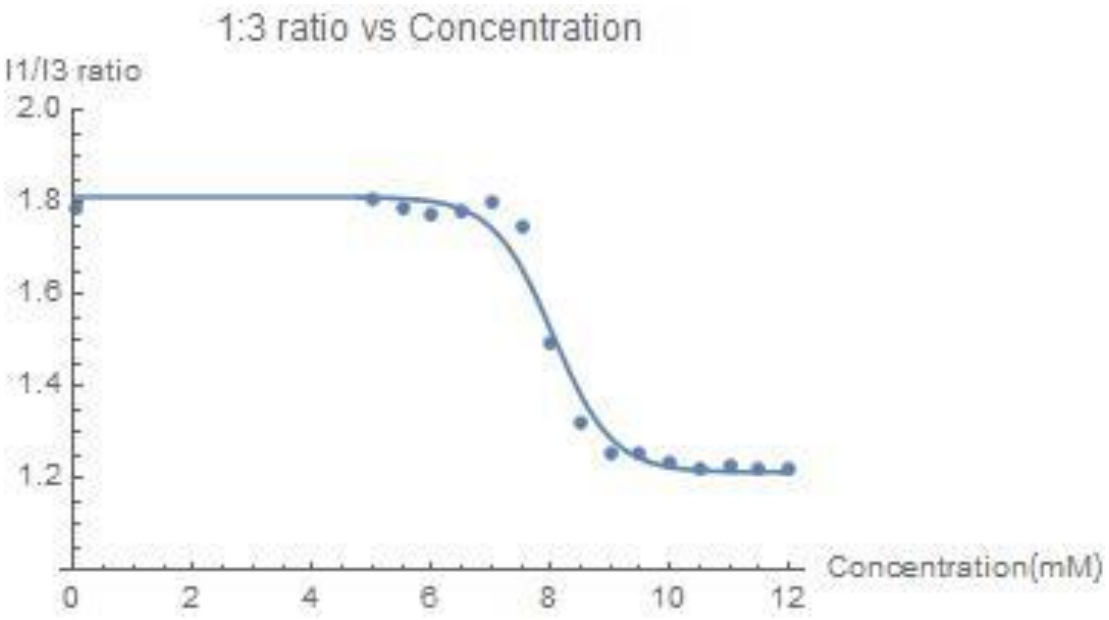

Figure 17 The fitting result of 1:3 ratio of SDS.
The fitting equation is the sigmoidal equation (Equation 1), and the calculation of fitting is completed by Mathematica.

From **Figure 17**, it is visible that nearly all the 1:3 ratio points are fitting the Sigmoidal Equation, which indicates that the CMC value calculated here is correct according to the principle of the 1:3 ratio methods. In addition, according to the calculation result, the CMC value of SDS here is 8.03 mM and the CMC value of SDS is 8.2 mM according to the reference[24]. Since these two value of CMC is close, it is concluded that the 1:3 ratio method utilized here is feasible for future experiments.

3.3.1.2. The effects of time after sonication on emission spectra and the 1:3 ratio

According to the methods of measuring the 1:3 ratio for the specific lipidoid solution, it is necessary to sonicate the sample solution for 5 minutes before the measurement. Since the fluorescent property of pyrene is affected by the surrounded environment significantly, errors will be introduced if the sample solution is not in equilibrium, even after sonication. Thus, it is necessary to investigate the emission spectra and the 1:3 ratio at different times for the same sample solution after sonicating the sample solution.

(a)

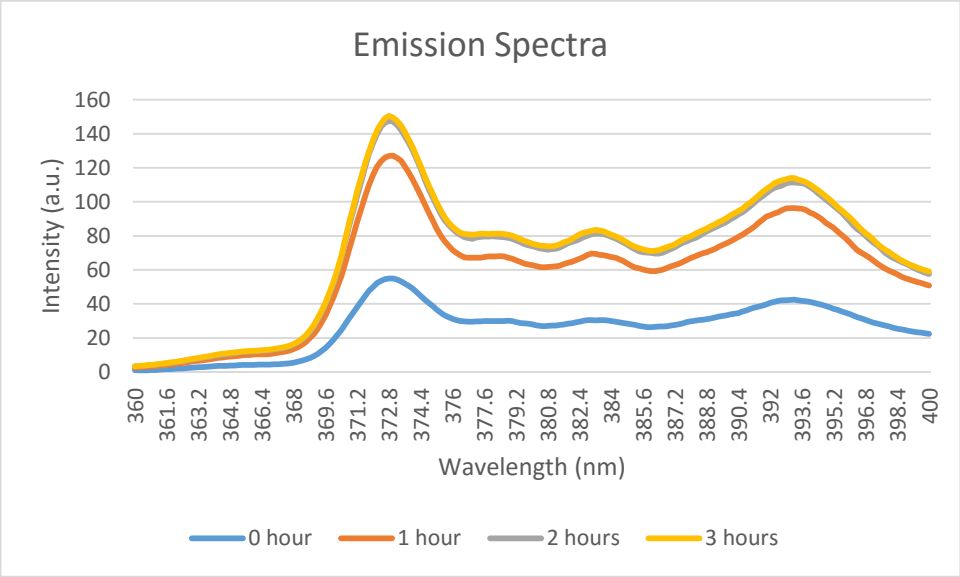

(b)

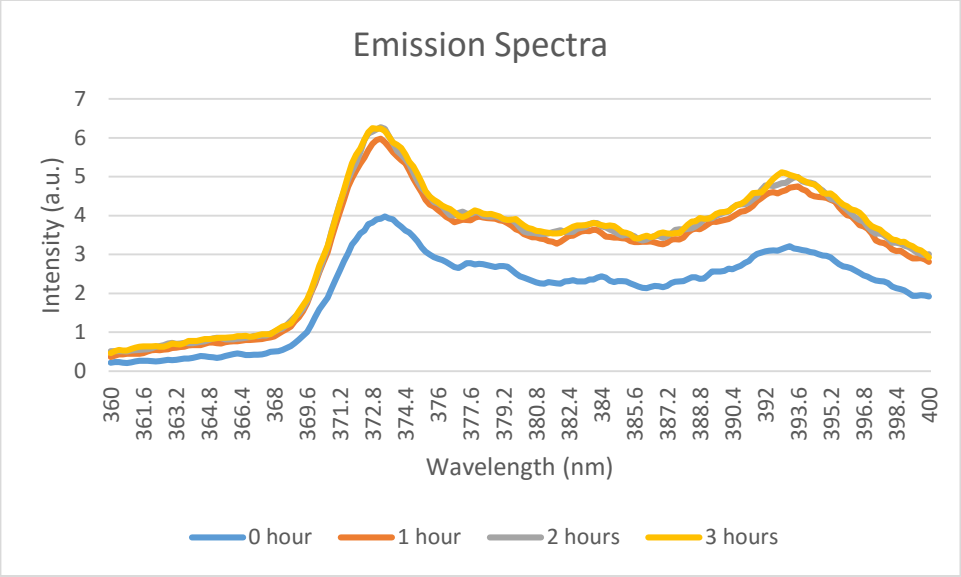

Figure 18 The emission spectrum of lipidoid (80O16B) solution at different times. (a)The concentration of lipidoid is 0; (b) the concentration of lipidoid is 0.05 mg/mL

From **Figure 18**, it is visible that as time increases, the emission spectrum is increasing, but the position of the peaks in the spectrum don't change. The changing pattern of the intensity of the first peak in **Figure 19** also profiles this.

(a)

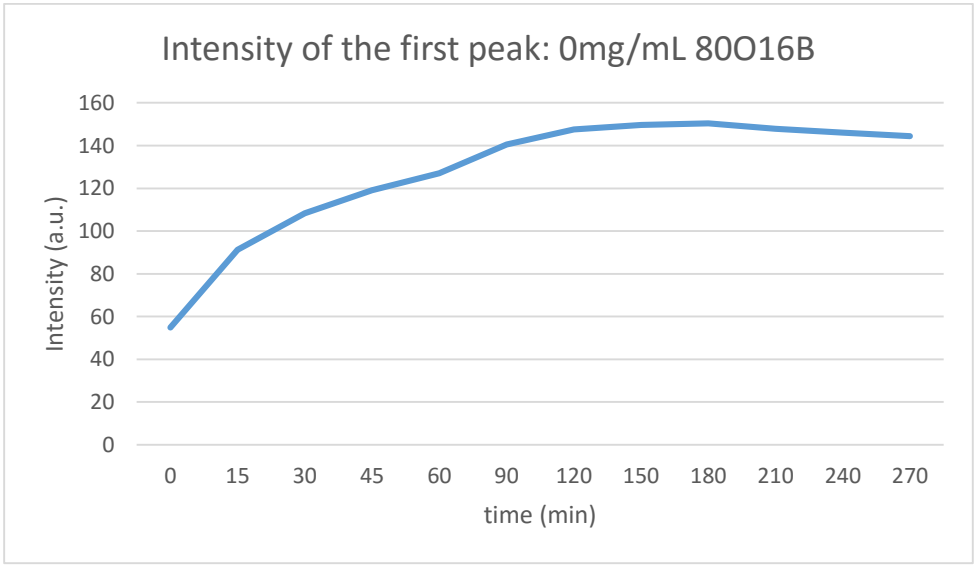

(b)

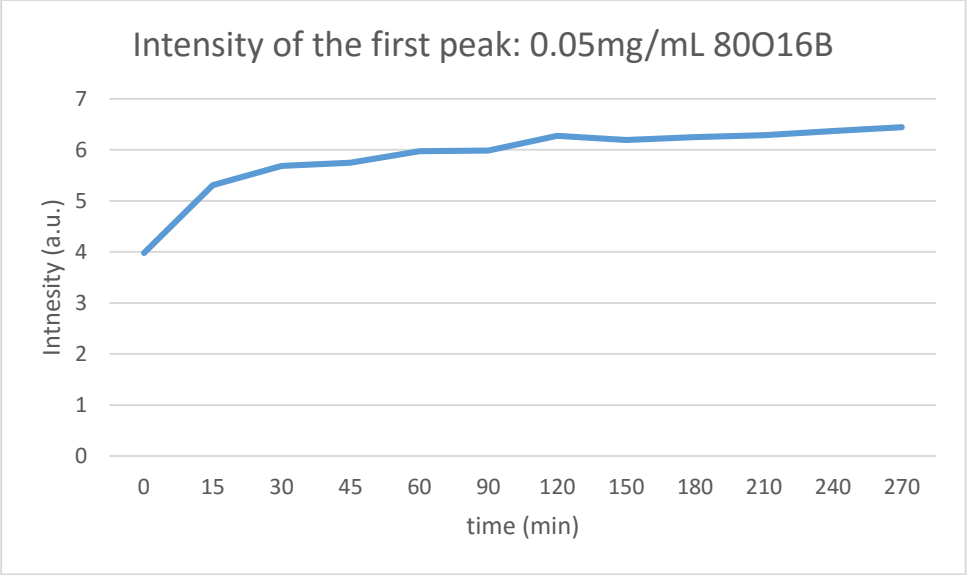

Figure 19 The change of the intensity of the first peak at different times.
(a)The concentration of the lipidoid (80O16B) is 0; (b)The concentration of the lipidoid (80O16B) is 0.05 mg/mL

Although the intensity of the emission spectrum will increase with the increase of time after sonication, the 1:3 ratio can be stable during the time period (See **Figure 20**), indicating that the stability of the 1:3 ratio can be maintained after sonication. As a result, the relative error can be ignored when measuring the CMC value of the lipidoids by 1:3 ratio method.

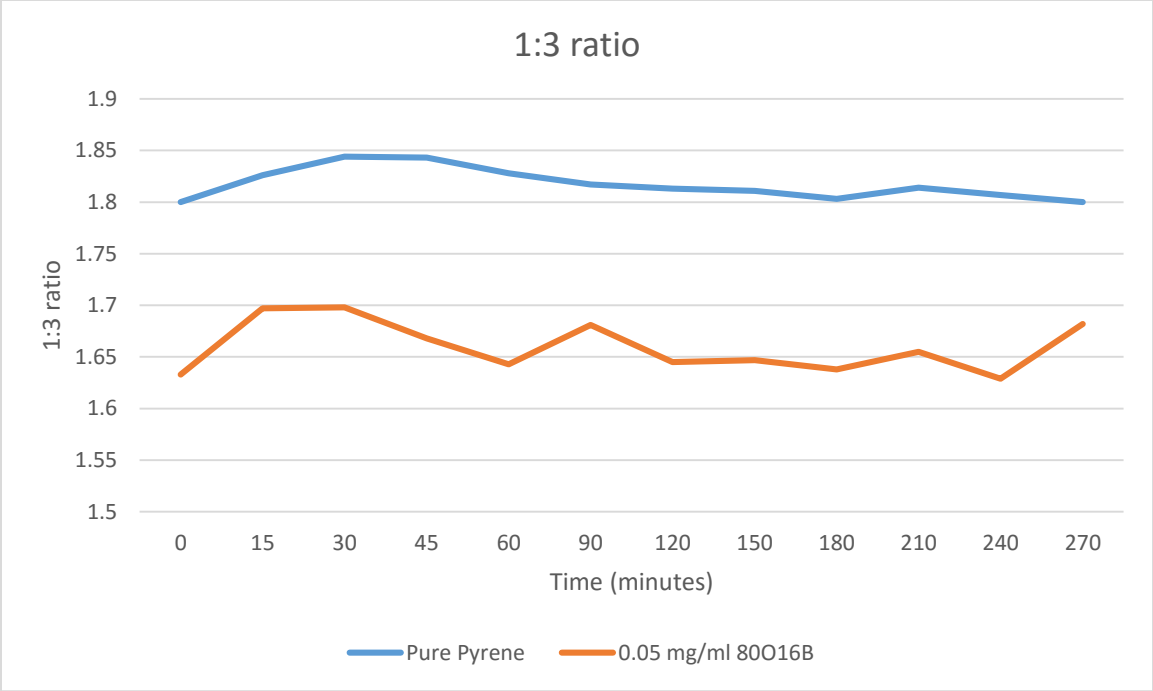

Figure 20 The change of 1:3 ratio of lipidoid at different concentrations with the increase of time

3.3.1.3. The effects of concentration of lipidoids

3.3.1.3.1. The effects of the concentration of the lipidoids on the emission spectra

According to the measurement of SDS and the reference, the intensity of the emission spectra of the surfactants will become larger with the increase of the concentration of the surfactant in the solution[22]. The intensity of the emission spectrum at the concentration above CMC value will be much larger than that of the emission spectrum at the concentration below the CMC value[34]. However, according to the analysis of the emission spectrum of the lipidoid solution, the result is in contrast (See **Figure 21**).

(a)

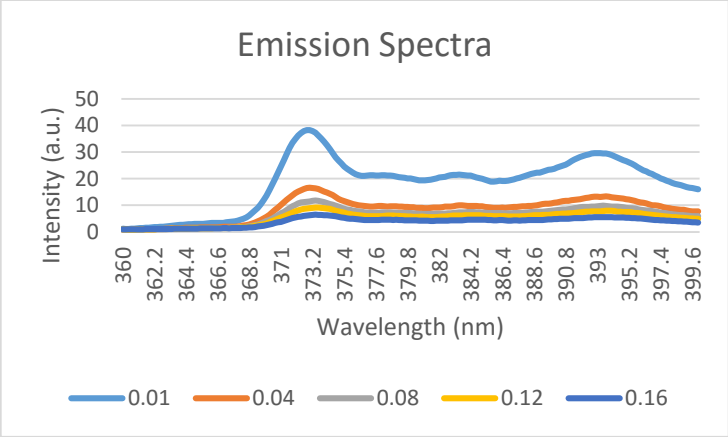

(b)

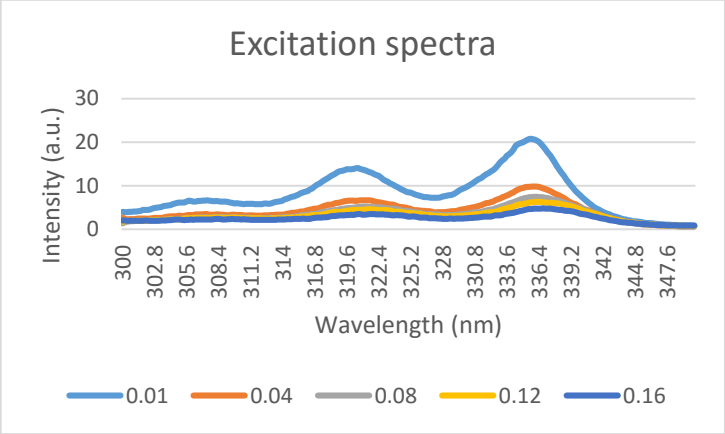

(c)

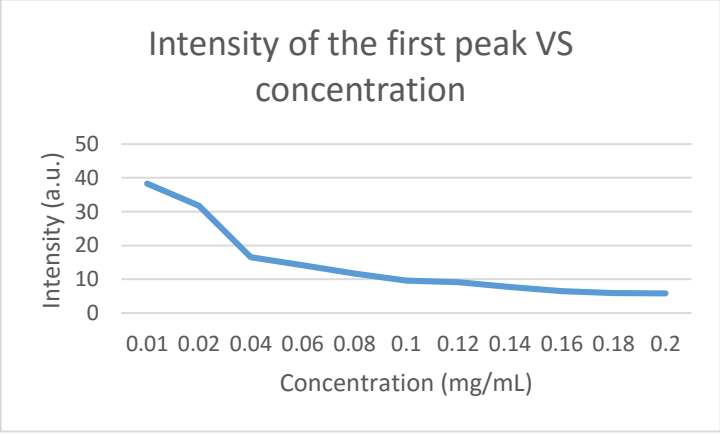

Figure 21 The effects of concentration of lipidoid (80O16B) on the spectrum.
(a) Emission spectrum (b) excitation spectrum (c) the intensity of the first peak with the increase of the concentration

Wilhelm et al believes that the changing pattern of the intensity of the peak at different concentrations is caused by the shift of the excitation and absorption spectrum[35]. However, **Figure 21** (b) has the same red shift pattern of the excitation spectrum as the reference, but the intensity in both of the emission spectrum and the excitation spectrum still decrease with the increase of the concentration of the lipidoids (See **Figure 21** (c)), which indicates that the red shift of the excitation spectrum is not the reason for the changing pattern of the intensity in emission spectrum. However, previous research which focused on the fluorescent quenching on pyrene led us to another possible explanation for the changing pattern of the intensity[36, 37]. Considering the electric charge of the nitrogen atoms in the amine groups, we think one possible reason for the decrease of the intensity in both of the emission and the excitation spectrum is that the amine groups in the lipidoid molecules can cause the fluorescence quenching of the pyrene in the solution.

3.3.1.3.2. The effects of the concentration of the lipidoids on the 1:3 ratio

According to the previous description of the mechanism of the 1:3 ratio method, it is expected that the 1:3 ratio will decrease with the increase of the concentration of the lipidoid during the measurement. The changing pattern of all the lipidoid molecules is expected to have the similar result (See **Figure 22**).

(a)

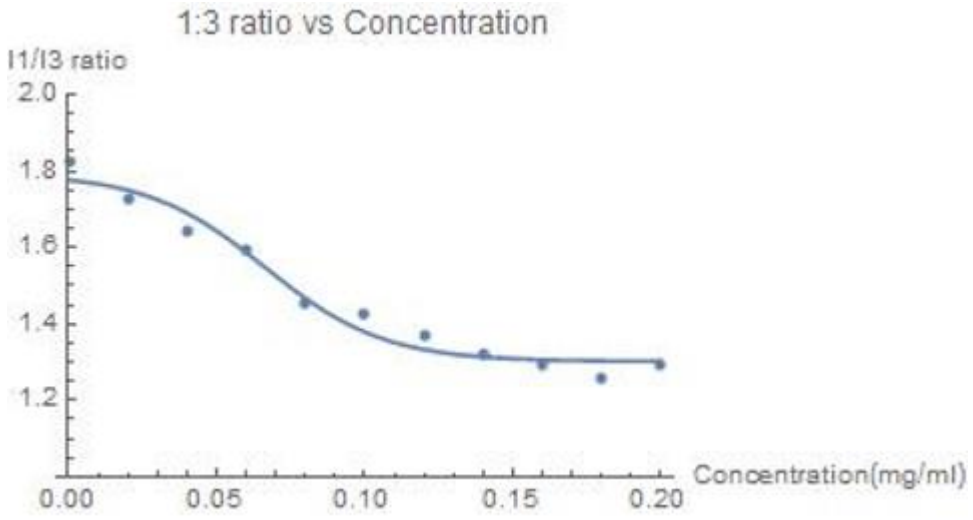

(b)

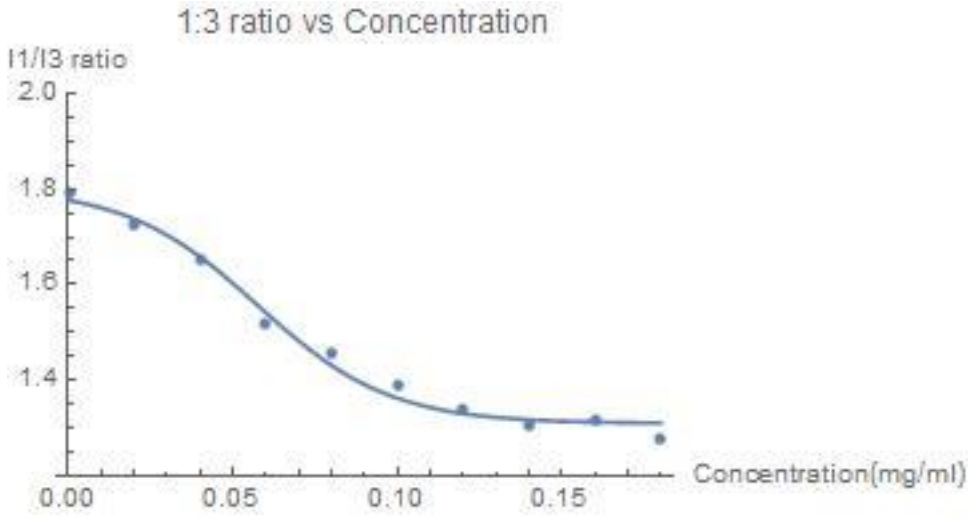

Figure 22 The 1:3 ratio of the lipidoids at different concentration
(a) The 1:3 ratio of 80O18B; (b) The 1:3 ratio of 87O16B

The changing pattern is close to the Sigmoidal Equation, so we can utilize the Mathematica to calculate the fitting result to the equation and get the CMC value of the specific molecule.

3.3.1.4. The effects of the structure of the lipidoids

3.3.1.4.1. The effects of the structure of the lipidoids on the 1:3 ratio

(a)

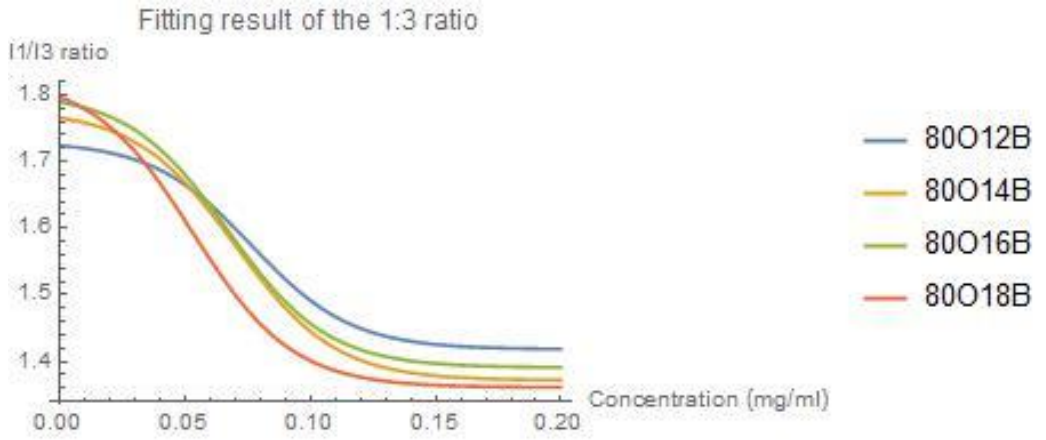

(b)

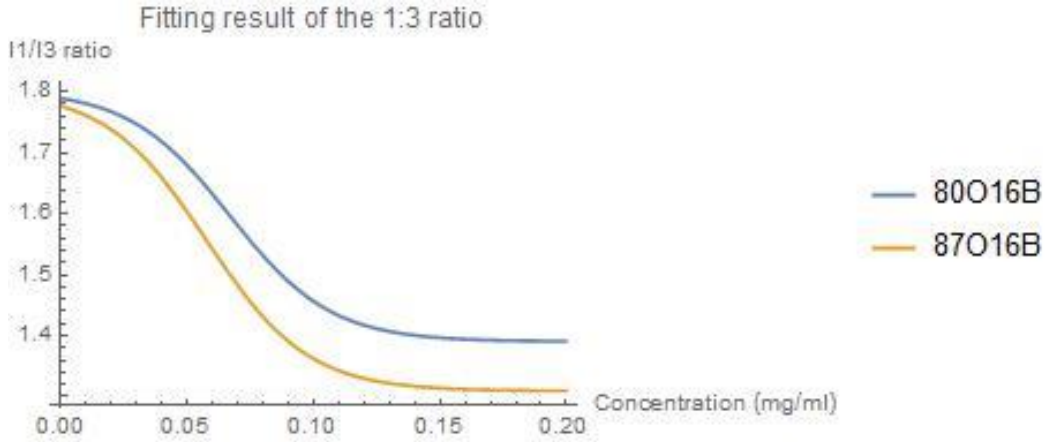

(c)

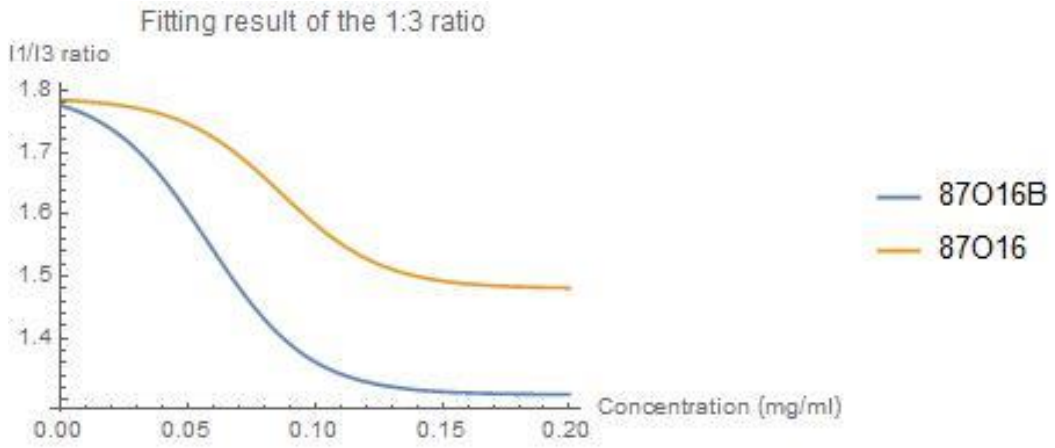

Figure 23 The fitting result of the 1:3 ratio for different lipidoids
(a)compare the lipidoids with different length of alkyl chain (b)compare the lipidoids with different head groups (c)compare the lipidoids with disulfide bond and the lipidoids without disulfide bond

Since the 1:3 ratio of the pyrene can indicate the polarity of the surrounding environment, which leads us to believe that the 1:3 ratio of the pyrene in the micelles can vary in different lipidoid solution. In order to investigate the hypothesis, we compared the fitting equation of different lipidoids (See **Figure 23**).

According to **Figure 23**, it is observed that the length of the chain has nearly no effects on the 1:3 ratio. However, the head group and the disulfide bond can affect the 1:3 ratio especially after micellization in the solution. To be specific, the existence of the disulfide bond will decrease the 1:3 ratio of the pyrene in the micelles and the lipidoids with “87” head group will also have lower 1:3 ratio in the micelle comparing to the lipidoids with “80” head group. This indicates that the polarity of the micelles formed by the lipidoids

with disulfide bond or the “87” head group is lower than that of the micelles formed by other lipidoids.

3.3.1.4.2. The effects of the structure of the lipidoids on the CMC value

According to the previous analysis, we utilize Mathematica to calculate the CMC value for all lipidoids and all the results are listed in the table and figure below (See **Table 3** and **Figure 24**):

Table 3 The CMC value of different lipidoids

	CMC (μM)		
	80 head group	87 head group	
	80B	87B	87
length of the chain	with disulfide bond	with disulfide bond	without disulfide bond
12	119	77.6	
14	96.7	69.6	
16	88.7	69.6	114
18	65.1	67.2	89.4

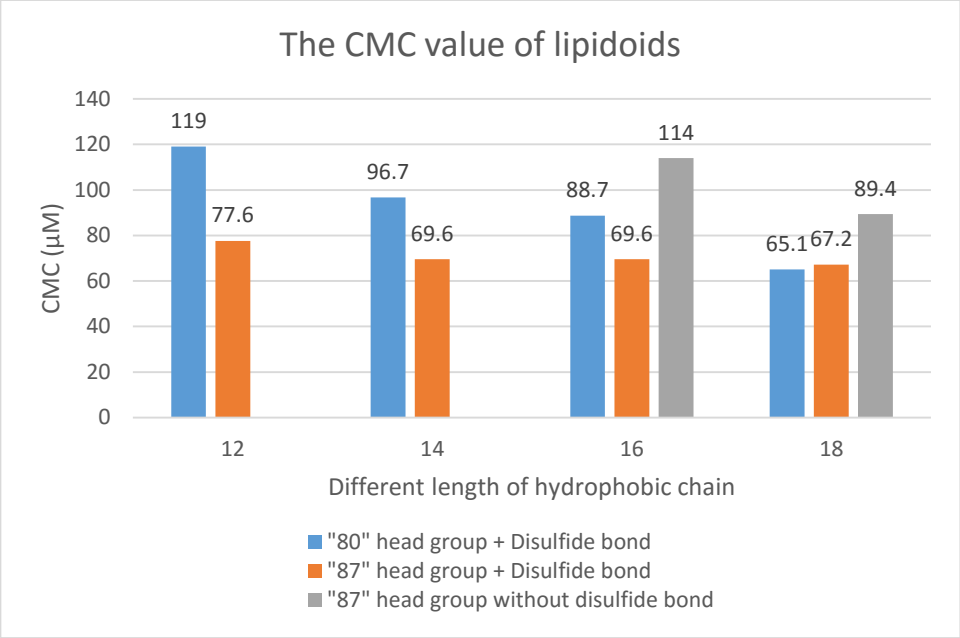

Figure 24 The comparison of CMC value of different lipidoids

Figure 24 indicates that there are three characteristics of the CMC value of lipidoids. First, with the increase of the concentration, the CMC value of the lipidoid will decrease. Second, the lipidoids with "87" head group have lower CMC value comparing to the lipidoids with "80" head group. Third, the lipidoid with disulfide bond will have lower CMC value comparing to the lipidoids without disulfide bond. According to these observations, we hypothesize that the CMC value can be affected by the structure of the lipidoid significantly. Since CMC value represents the tendency of surfactants in aqueous solution[38], it is concluded that the structure of the lipidoids can affect the capability of self-assembly of lipidoids in solution.

3.3.1.5. Summary

According to the analysis of the fluorescent results of the pyrene, it is concluded that:

1) 1:3 ratio method is a feasible method for measuring the CMC value of the lipidoids synthesized in our lab.
2) The length of the alkyl chain in the lipidoid can affect the self-assembly of the lipidoids, but not very significantly.
3) The head group and the disulfide bond can affect the tendency of self-assembly significantly according to the comparison of the CMC value at the micellization stage.
4) According to the comparison of 1:3 ratio and the previous conclusion, we can find that the tendency of self-assembly is related to the polarity of the inner space of the micelles. If the inner space of the micelle has lower polarity (low 1:3 ratio), the corresponding lipidoids will have stronger tendency for self-assembly.

3.3.2. Characterization of morphology of micelles of lipidoids by using AFM

As a microscopy technique with high resolution, AFM can provide direct observation on the morphology of the micelles. Thus, AFM has been widely used in the research of micelles formed by different surfactants such as polymeric micelles[39], milk casein micelles[40], etc. With the comparison of the morphology between different lipidoids by AFM, it can be helpful to investigate the relationship between the micellization behavior of the lipidoids and their structure. **Figure 25** indicates the micelles formed by two different lipidoids at the same concentration (1 mg/mL).

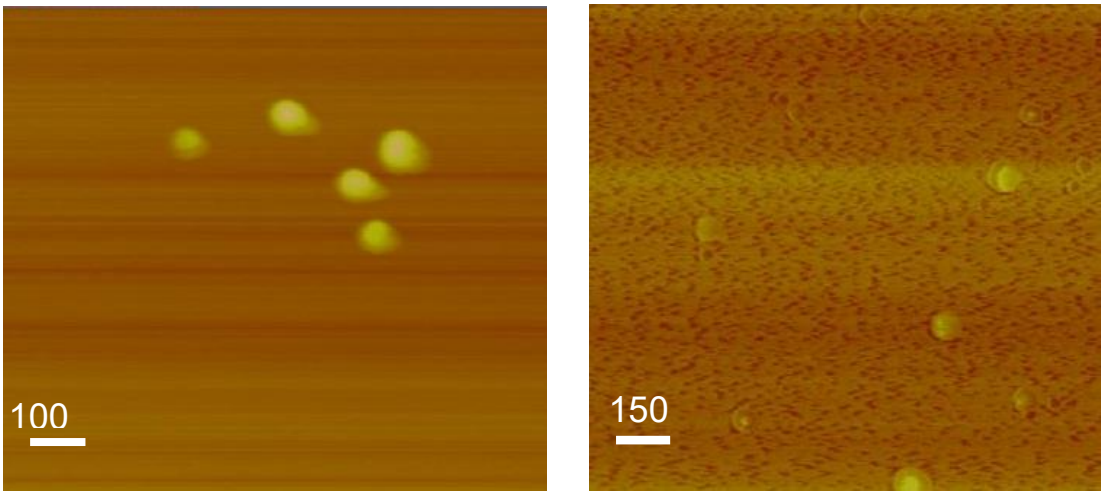

(a) (b)

Figure 25 The height image of different lipidoids through AFM
(a) 87O16B (b) 80O16

In **Figure 25**, the shape of the micelles can be observed, indicating that both of these two lipidoids have formed spherical micelles at 1 mg/mL. In other words, the CMC value of the lipidoids should be lower than 1 mg/mL which has been proved by the 1:3 ratio method. The radius of these micelles were calculated for further calculation (See **Table 4**).

Table 4 The radius of the micelles of different lipidoids

Lipidoid	*87O16B*	*80O16*
Average Radius (nm)	80.86	67.6
Standard Deviation (nm)	20.09	13.97

According to **Table 4**, it is concluded that the radius of the micelle formed by 87O16B is much larger than that of the 80O16. Considering the difference of the CMC value and the 1:3 ratio caused by the structure of these two lipidoids, further investigation of the relationship between the radius of the micelles and the corresponding CMC value and the 1:3 ratio is required, which will be emphasized in the future direction section.

Chapter 4 Study of self-assembly of lipidoids by molecular simulation

4.1. Introduction

4.1.1. Background

Molecular Modeling represents several different methods which can calculate and mimic the behavior of the molecules in different scales of the systems with the assistance of computer science. With the development of computer engineering, computer performance has become more powerful than in the past. Even a personal laptop can complete some simple molecular simulation. On the other hand, the research of the molecular behavior has become more difficult with the restriction of modern techniques. The role of molecular modeling in modern molecular research area has become more important. According to the basic principle utilized during the simulation, molecular modeling can be divided into two different classes: molecular dynamics (MD) and Monte Carlo (MC)[41]. There are also many hybrid techniques which combine the features of these two methods together.

The process of Molecular Dynamics (MD) is very similar to the real experiment. Researchers prepare the files that include the coordinates and the force fields of the

sample before the experiment. Then, Newton's equation of motion will be applied for the whole system with the increase of time, making it convenient to observe the motion of all the molecules from the beginning of the simulation to the equilibrium state of the system[41].

Monte Carlo (MC) has a very different principle compared to MD. For example, the algorithm of Metropolis method which is widely used in MC is stated as following: First, select the particle from the system at random and calculate its energy. Then, give this particle a random displacement and calculate its energy again. Finally, according to its new energy and the previous energy, there is a probability to determine whether to accept this displacement[41].

With the description of these two methods, it can be concluded that MD has an advantage over MC, because MD can profile the property of the system in a dynamical way and researchers can observe the state of the system at the specific time[42]. Thus we selected to utilize MD method for simulating the lipidoids' behavior.

4.1.2. Introduction of software

The software we used for the molecular dynamic simulation includes: NAMD, VMD, Spartan, and packmol.

NAnoscale Molecular Dynamics (NAMD) program is a free software for molecular dynamic simulation based on Charm++ parallel programming language. It was invented by Nelson in 1996 at the University of Illinois as an object-oriented, parallel MD program[43]. It has several advantages as a molecular dynamics simulation program. First, it is free and its source code is also free for non-commercial use, which will decrease the cost for molecular simulation. Second, as a parallel program, NAMD can run the simulation on multiple processors in a parallel way, which will decrease the simulation time. Finally, the latest version of NAMD has been able to simulate a very large system. For example, Villa et al have completed a simulation system which is multiscale LacI-DNA complex with 314,000 atoms for more than 10 ns on hundreds of processors[44].

Visual Molecular Dynamics (VMD) is a visualization software for molecular simulation. It has several functions for simulation. First, it can be used to observe the static structure of the molecules visually and analyze the related data with different plugins. Second, it can also read the trajectory file of the simulation system and analyze the trajectory of the molecules, including the RMSD calculation, energy calculation, temperature distribution, etc. Third, through IMD connect function with NAMD during simulation, users can complete the interactive molecular dynamic simulation such as applying forces to the system in a specific direction[45, 46].

Figure 26 NAMD can be utilized for Interactive Molecular Dynamic Simulation[46]

Spartan is a molecular simulation software from Wavefuncion. Its primary function is to build the molecule according to its structural formula and export the files with the coordinates of all atoms in the molecules which can be utilized in the simulation. It is necessary to minimize the energy of the molecule before exporting the coordinate files which is called mol2 file.

Packmol is utilized for preparing the coordinate files before the simulation. It can create the initial position for multiple molecules in the determined space and make sure that the short range repulsive will not cause the disruption of the simulation[47]. On the other hand, we need to investigate the interaction among multiple molecules through molecular dynamics (MD), but Spartan can only provide the coordinate file of a single molecule. As a result, it is necessary to find a way to arrange the multiple molecules in the determined area and add water molecules and ions into the system, so we utilized packmol to replicate the lipidoid molecule and arranged them at random in the determine space such

as a box. According to each model we used for simulation, we use packmol to add water molecules and ions into the system as well.

4.1.3. Simulation detail

4.1.3.1. Simulation models

4.1.3.1.1. Implicit Solvent Model

General Born Implicit Solvent (GBIS) model is a relatively faster model for simulation, because it allows the simulation to work without explicit solvent water molecules in the system, which can decrease the number of atoms in the system[48].

Since the GBIS model can accelerate the speed of the simulation, we utilize GBIS model at first for our simulation.

4.1.3.1.2. Explicit Solvent Model

In contrast to the GBIS model which has only implicit solvent molecules such as water molecules in the system, another way to complete the simulation on NAMD is adding explicit water molecules and ions to surround the lipidoid molecules to make them solvated in the system like a large water box.

4.1.3.2. Periodic Boundary Condition

Since the scale of the real system is usually much larger than that of the simulation system, it is necessary to use a small and finite system to replace the real system in simulation. However, the atoms near the boundary of the simulation system will be affected by the surface effects, which will cause the failure of the simulation. In order to avoid the surface effects, periodic boundary condition (PBC) is utilized.

In periodic boundary condition, all the atoms in the system are thought to have many images around the simulation system. The distance between the image and the original atoms are always the same, and this distance is equal to the length of the simulation system in that direction. These images have the same motion as the original atoms, so when the original atoms move to the surface of the simulation system, there must be another image of these atoms moving closer to the surface of the simulation system at the opposite direction. When these atoms move to the outside of the simulation system, there must be an image as they move into the simulation system at the opposite side with the same velocity and orientation (See **Figure 27**). In this way, the surface effects can be avoided and the infinite simulation system can be replaced by a finite simulation system.

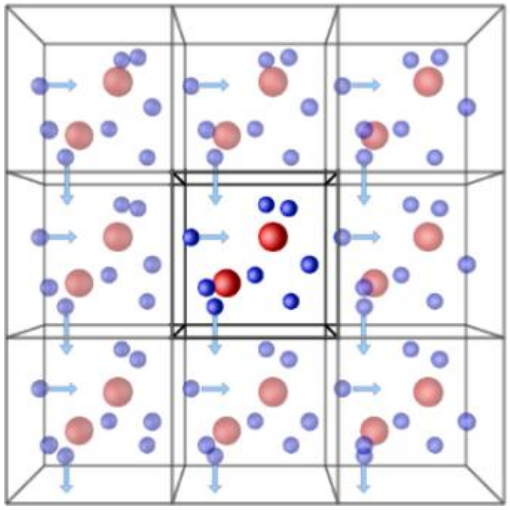

Figure 27 The Periodic Boundary Condition (Source: http://isaacs.sourceforge.net/phys/pbc.html)

4.1.3.3. Analysis of the equilibrium state of the system

4.1.3.3.1. RMSD data

Root Mean Square Deviation (RMSD) is a method to measure the difference between different frames of the same residue in the molecules. It is defined as:

$$\mathrm{RMSD} = \sqrt{\frac{1}{N}\sum_{i=1}^{N}\delta_i^2} \qquad (2)$$

Where δ is the distance between the same atom in different frames in the trajectory file and N is the number of atoms selected for calculating the RMSD data. In order to indicate the equilibrium state of the system, RMSD data represents the difference between the atoms in the specific frame and the initial state. At the beginning of the simulation, this RMSD will increase because of the motion of the atoms in the simulation. However, with

the increase of the time, when the system is in equilibrium state, the RMSD data will keep stable. That's how RMSD can be used to profile the equilibrium state of the simulation.

4.1.3.3.2. Total Energy

The total energy here is the sum of different potential energies and the kinetic energy in the simulation. The total energy is recorded in the log file during the simulation and can be used to indicate the equilibrium state of the system (See **Figure 28**).

ETITLE:	TS	BOND	ANGLE	DIHED	IMPRP
	ELECT	VDW	BOUNDARY	MISC	KINETIC
	TOTAL	TEMP	TOTAL2	TOTAL3	TEMPAVG
	PRESSURE	GPRESSURE	VOLUME	PRESSAVG	GPRESSAVG
ENERGY:	1000	0.0000	0.0000	0.0000	0.0000
	-97022.1848	9595.3175	0.0000	0.0000	14319.5268
	-73107.3405	300.2464	-73076.6148	-73084.1411	297.7598
	-626.5205	-636.6638	240716.1374	-616.5673	-616.6619

Figure 28 The data format including energy of the system at the specific timestep in the log file[49]

4.1.3.3.3. Temperature Fluctuation

Since the temperature will maintain stability at the equilibrium state, it is necessary to check the distribution of the temperature in the system during the simulation. If the distribution of the temperature at the equilibrium state is nearly a normal distribution, then we can conclude that the system in the equilibrium state.

4.2. Software and Methods

4.2.1. Software and simulation files

4.2.1.1. The simulation files

As previous description of the Molecular Dynamics (MD) simulation, users have to prepare all the necessary files before the simulation like performing a real experiment. In order to conduct the simulation through NAMD, several files are required: pdb file, psf file, parameter files and a configuration file[49].

4.2.1.1.1. Protein Data Bank (pdb) file

The Protein Data Bank is a worldwide archive of the structural information for the biological macromolecules. The uniform format includes the information of the atomic coordinates for the specific molecule and will mark the different residue of this molecule with labels for farther computation[50, 51]. Here we utilize the software Spartan 10 to export the mol2 file directly, then VMD can be used for exporting the pdb file from the mol2 file.

```
ATOM      1  N   MET     1      27.340  24.430   2.614  1.00  9.67      1UBQ  71
ATOM      2  CA  MET     1      26.266  25.413   2.842  1.00 10.38      1UBQ  72
ATOM      3  C   MET     1      26.913  26.639   3.531  1.00  9.62      1UBQ  73
ATOM      4  O   MET     1      27.886  26.463   4.263  1.00  9.62      1UBQ  74
ATOM      5  CB  MET     1      25.112  24.880   3.649  1.00 13.77      1UBQ  75
ATOM      6  CG  MET     1      25.353  24.860   5.134  1.00 16.29      1UBQ  76
ATOM      7  SD  MET     1      23.930  23.959   5.904  1.00 17.17      1UBQ  77
ATOM      8  CE  MET     1      24.447  23.984   7.620  1.00 16.11      1UBQ  78
ATOM      9  N   GLN     2      26.335  27.770   3.258  1.00  9.27      1UBQ  79
ATOM     10  CA  GLN     2      26.850  29.021   3.898  1.00  9.07      1UBQ  80
ATOM     11  C   GLN     2      26.100  29.253   5.202  1.00  8.72      1UBQ  81
ATOM     12  O   GLN     2      24.865  29.024   5.330  1.00  8.22      1UBQ  82
ATOM     13  CB  GLN     2      26.733  30.148   2.905  1.00 14.46      1UBQ  83
ATOM     14  CG  GLN     2      26.882  31.546   3.409  1.00 17.01      1UBQ  84
ATOM     15  CD  GLN     2      26.786  32.562   2.270  1.00 20.10      1UBQ  85
ATOM     16  OE1 GLN     2      27.783  33.160   1.870  1.00 21.89      1UBQ  86
ATOM     17  NE2 GLN     2      25.562  32.733   1.806  1.00 19.49      1UBQ  87
```

Figure 29 The format of PDB file[49]. This pdb file include the number of the atom, the residue name, the number of the chain, the coordinates, etc.

4.2.1.1.2. Protein Structure File (psf)

The Protein Structure File (psf) file contains the structural information of the macromolecule such as the bonding interaction. With the help of the plugin (psfgen) in the VMD, the psf file can be exported according to the specific pdb file and the parameter files.

4.2.1.1.3. Parameter file

The parameter files usually store the force field according to the system experience. It can be utilized to calculate the potential of the specific atom during the simulation[52]. What we used here is the CHARMM force field and the most of the related parameter files can be downloaded from the website (http://mackerell.umaryland.edu/index.shtml).

However, we still need to generate a parameter files according to the mol2 file for the specific molecule. This file is called str file which contains the information of the topology of the specific molecule and it can be exported on the website of ParamChem (https://cgenff.paramchem.org/)

4.2.1.1.4. Configuration file

The configuration file contains all the options such as the selection of the parameter files, the type of the model, and the size of the periodic boundary condition for NAMD when running the simulation.

4.2.1.2. The necessary software

4.2.1.2.1. Spartan 10

Spartan 10 is utilized for constructing the coordinates file of the specific lipidoid and minimizing the energy of the molecule before exporting the coordinate file.

4.2.1.2.2. VMD

VMD is utilized for two functions:

First, observe the trajectory of the molecules of the simulation.

Second, export the pdb file and psf file with the specific plugin.

4.2.1.2.3. NAMD

NAMD is the simulation program. It will read the configuration file and complete the simulation.

4.2.1.2.4. ParamChem

ParamChem is utilized to export the specific parameter file according to the mol2 file exported from Spartan 10.

4.2.1.2.5. Packmol

Packmol is utilized to replicate the molecules and distribute the molecules according to the requirement of the simulation.

4.2.1.2.6. Tufts Research Cluster

Tufts Research Cluster is a high performance computing server and was used to perform the simulation with the NAMD installed on it.

4.2.2. Method

4.2.2.1. The simulation model for the aggregation of the lipidoid molecules

In this simulation model, we will arrange the molecules in a determined region at random and check the aggregation of them.

1) Prepare the pdb file and the parameter files including the str file for the single lipidoid as previous description.
2) Replicate the single molecules and distribute them in a determined region at random through Packmol. Add the water molecules and the ions if the model includes the explicit solvent molecules. Then export the pdb file for the system of the multiple molecules.
3) Read the pdb file with multiple molecules into VMD and generate the corresponding psf file with the psfgen plugin.
4) Write the configuration file for the simulation system.
5) Upload the simulation files onto Cluster and run the simulation. Then analyze the trajectory and log file after the simulation.

4.2.2.2. The simulation model for the bilayer structure of lipidoid molecules

In this simulation model, we will arrange the molecules to form a bilayer structure and check stability of the bilayer structure.

1) Prepare the pdb file and the parameter files including the str file for the single lipidoid as previous description.
2) Replicate the single molecules and arrange these molecules to form a bilayer structure through Packmol. Add the water molecules and ions if the simulation model includes the explicit solvent molecules. Then export the pdb file for the system of the bilayer structure.
3) Read the pdb file with multiple molecules into VMD and generate the corresponding psf file with the psfgen plugin.
4) Write the configuration file for the simulation system.
5) Upload the simulation files onto Cluster and run the simulation. Then analyze the trajectory and log file after the simulation.

4.3. Results and Discussion

4.3.1. Results

4.3.1.1. The simulation model for the aggregation of the lipidoids

In order to conduct the simulation of the aggregation of the lipidoids in the solvent, we utilized the simulation model with implicit solvent molecules (GBIS model) at first, then added explicit water molecules and the ions in the system.

4.3.1.1.1. The implicit solvent model

The simulation started with 30 molecules which were distributed at random in a periodic boundary condition (80 × 80 × 80 A) and ended after 4 ns. The initial distribution and the final distribution of one lipidoid 87O18B is as following:

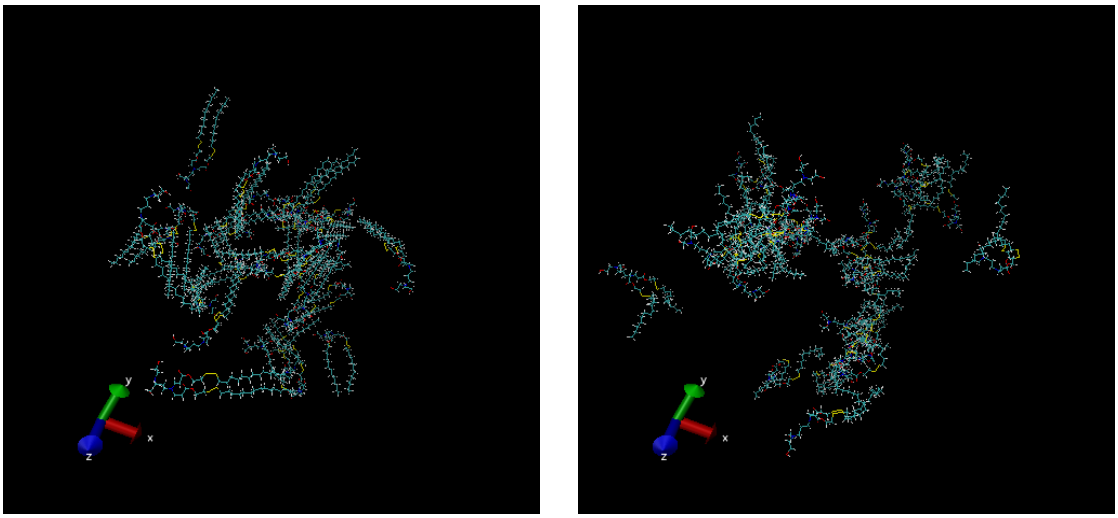

(a) (b)

Figure 30 The initial state and the final state of the aggregation simulation by implicit solvent model (87O18B)
(a) initial state (b) final state

Figure 30 indicates that the molecules can aggregate together after 4ns in the simulation system. However, it is clear that the aggregation of the lipidoids is not very close and that these molecules have formed several clusters in the system.

The RMSD data of the system indicates that they have been in equilibrium state (See **Figure 31**), which means that the aggregation state of the molecules will not change much with the increase of time.

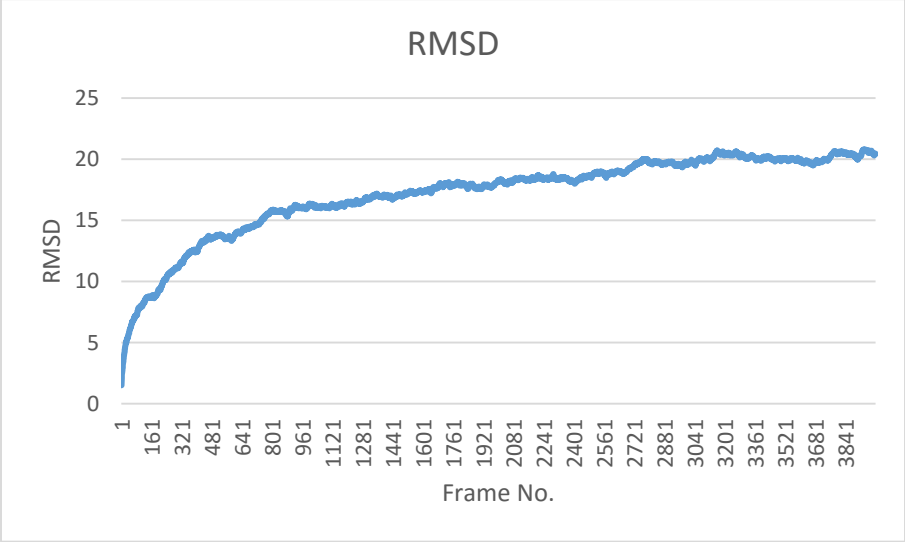

Figure 31 The RMSD data of the whole lipidoids (87O18B) for the simulation of the implicit solvent model

4.3.1.1.2. The explicit solvent model

The simulation with explicit solvent molecules started with 30 molecules which were distributed with water molecules and ions at random in a determined region (80 × 80 × 80 A) and the simulation lasted for 4 ns. With the comparison between the initial state

and the final state of 87O18B (See **Figure 32**), it is concluded that the molecules can aggregate in the solution.

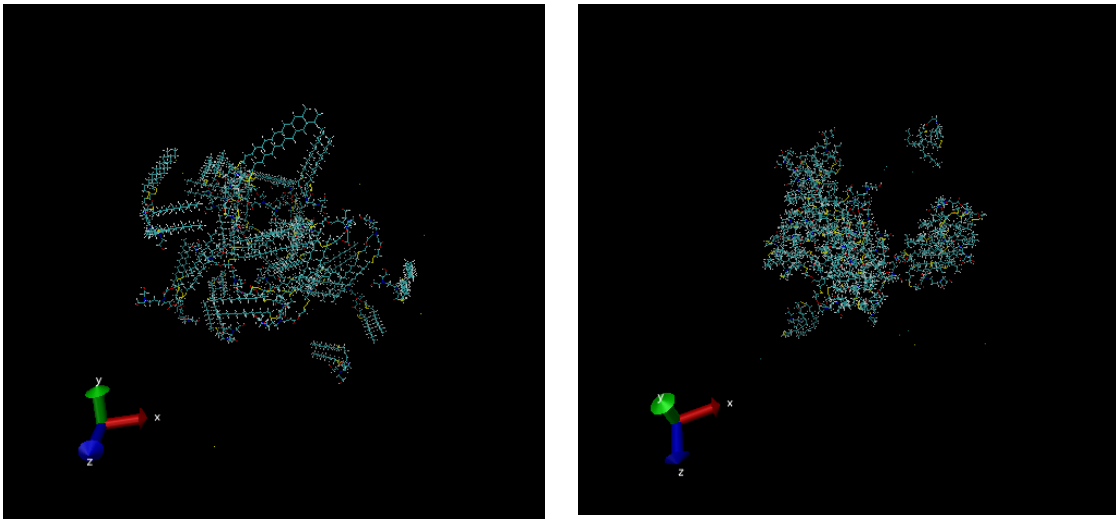

(a) (b)

Figure 32 The initial state and the finals state of the aggregation simulation of lipidoids (87O18B) by explicit solvent model
(a) initial state (b) final state

Though both of these two simulations have the aggregation of 30 same lipidoids in 4 ns, their behaviors are not the same. It can be easily concluded that the aggregation of lipidoids in the system with explicit water molecules is much better than that of the system with implicit water molecules, which indicates that there exist differences between these two different models during the simulation.

In addition, according to the RMSD data, the total energy and the temperature fluctuation of the system (See **Figure 33**), it is clear that the system has been in equilibrium state.

(a)

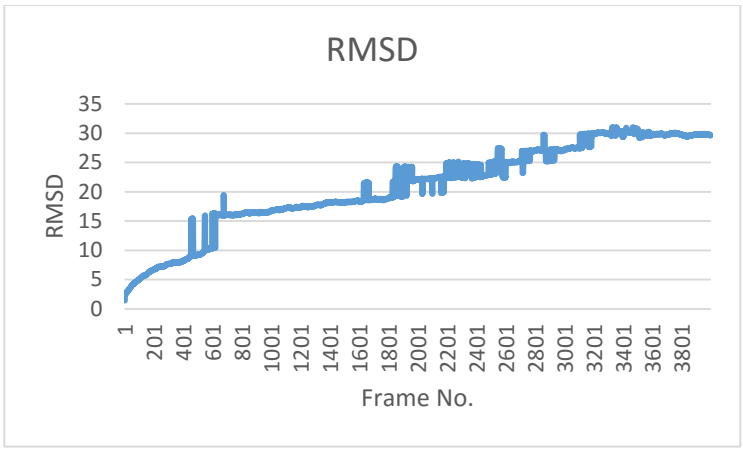

(b)

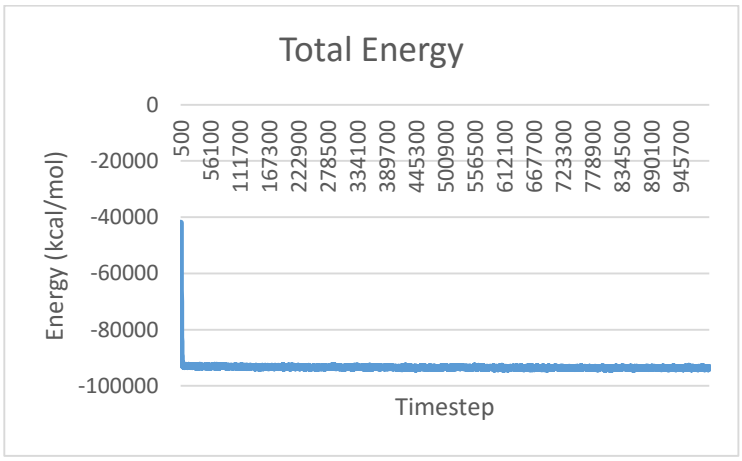

(c)

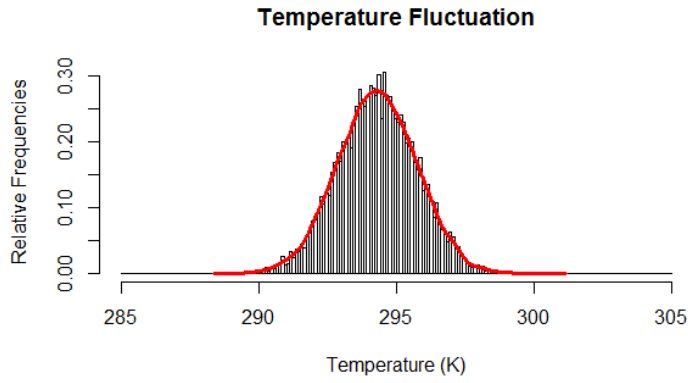

Figure 33 The equilibrium state of the system (87O18B)
(a) RMSD data (b) Total energy (c) Temperature fluctuation

4.3.1.2. The simulation model for the bilayer structure of the lipidoids

In order to conduct the simulation of the bilayer structure of the lipidoids in the solvent. We utilized the simulation model with implicit solvent molecules (GBIS model) at first, then added explicit water molecules and the ions in the system to simulate the real aggregation system.

4.3.1.2.1. The implicit solvent model

The bilayer structure was composed of 40 lipidoids and each side had 20 lipidoids. The area of the bilayer was 40 × 40 A and the depth of the whole bilayer was twice of the length of the lipidoid. The simulation lasted for 4 ns in GBIS model and the result is as following:

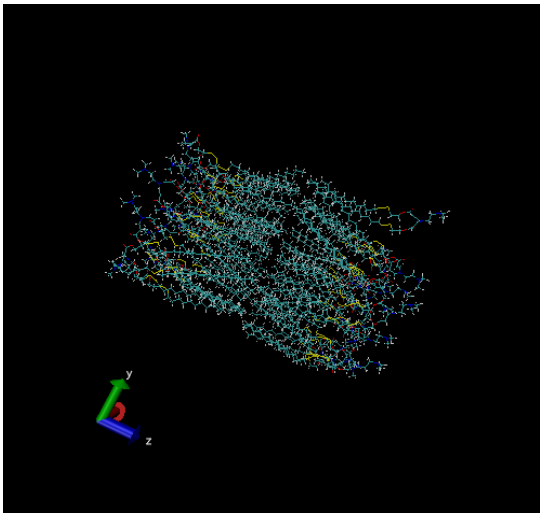

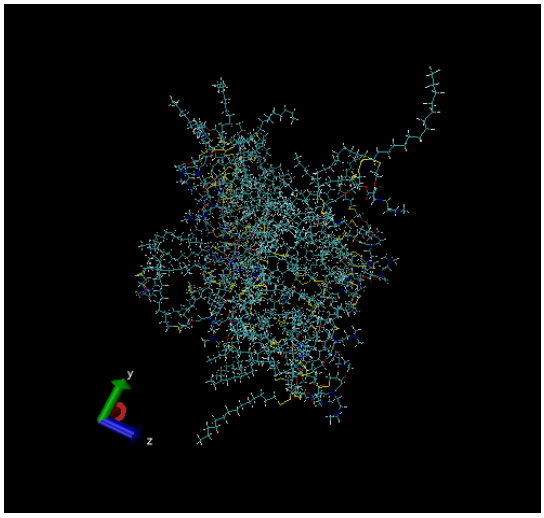

(a) (b)

Figure 34 The initial state and the final state of the simulation of 80O18B by an implicit model
(a) initial state (b) final state

From **Figure 34**, it is visible that the structure of the bilayer has been disrupted completely after the simulation of 4 ns. Considering the RMSD data, total energy and the temperature fluctuation of the system in **Figure 35**, this system has been in equilibrium state, indicating that the bilayer structure won't be rebuilt with the increase of the time.

(a)

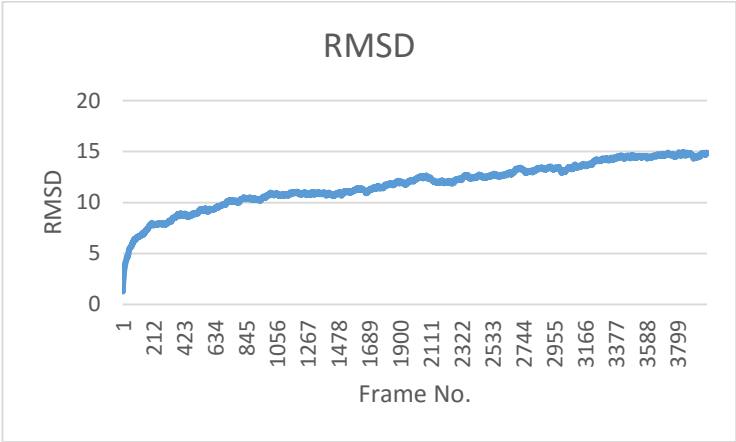

(b)

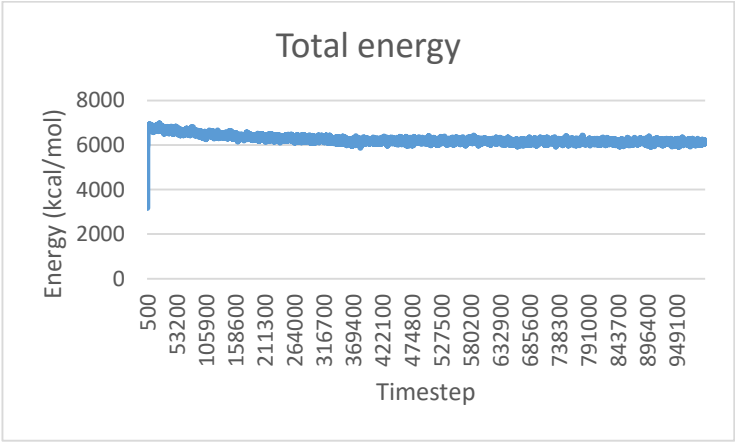

(c)

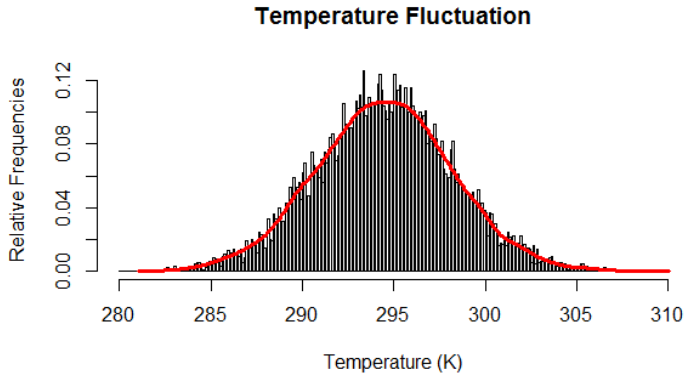

Figure 35 The equilibrium state of the system (80O18B)
(a) RMSD data (b) Total energy (c) Temperature fluctuation

4.3.1.2.2. The explicit solvent model

In the explicit solvent model of the bilayer structure, the water molecules and the ions were added on each side of the bilayer to simulate the bilayer structure in the buffer solution. The simulation lasted for 4 ns as well and the result is as following:

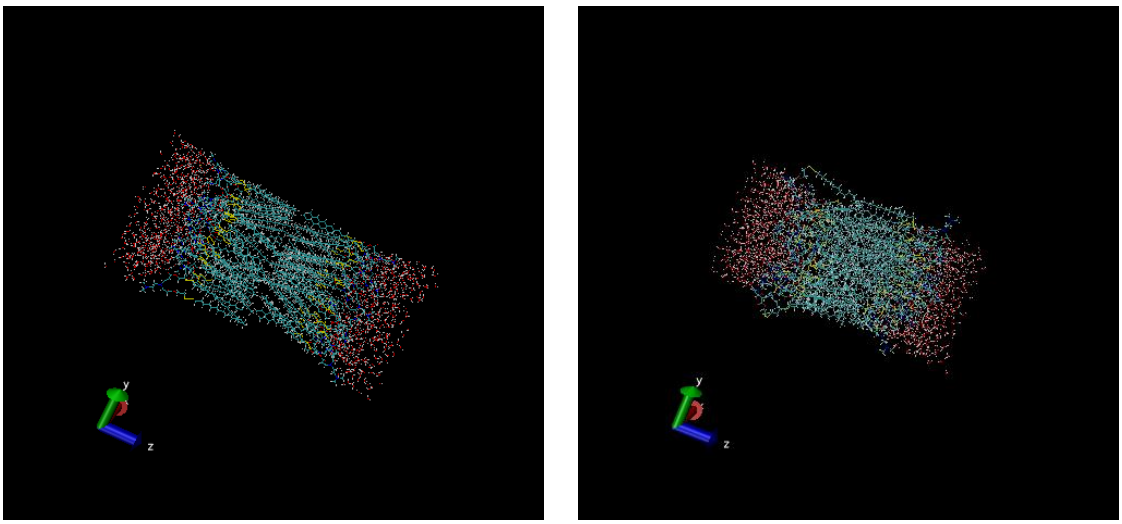

(a) (b)

Figure 36 The initial state and the final state of the simulation (80O18B) by the explicit model
(a) initial state (b) final state

It is visible that the bilayer structure can keep stable after 4 ns of simulation. Then the RMSD data, total energy and the temperature fluctuation of the system were also checked in **Figure 37**.

(a)

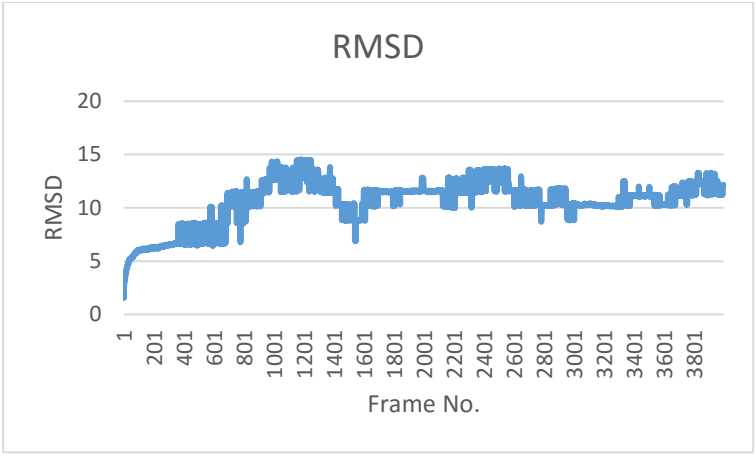

(b)

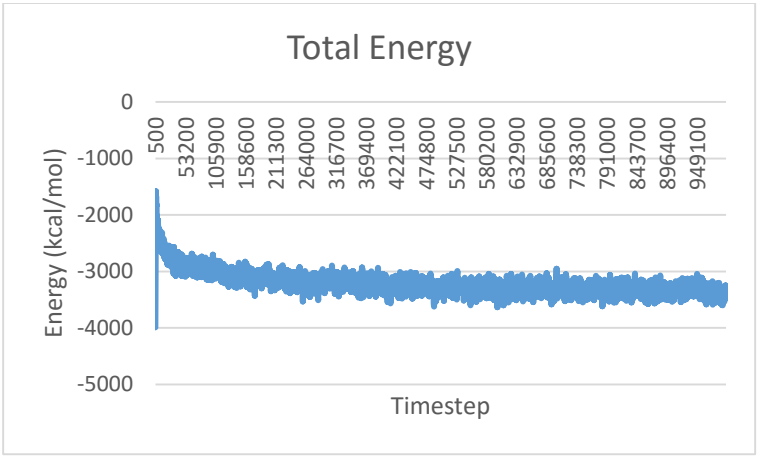

(c)

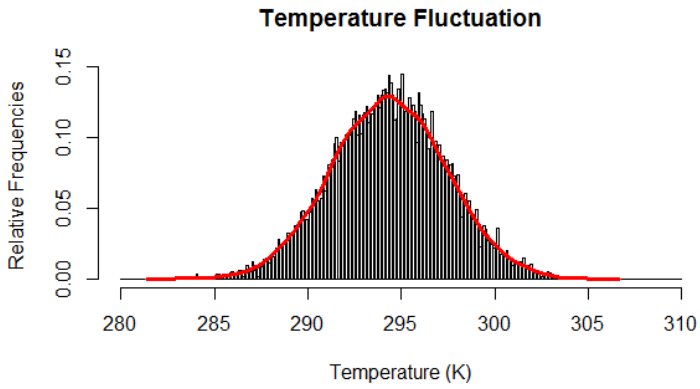

Figure 37 The equilibrium state of the simulation system (80O18B)
(a) RMSD data (b) Total energy (c) Temperature fluctuation

Figure 37 indicates that the system has been in equilibrium state and that the bilayer structure can maintain stability with the increase of the time.

4.3.2. Discussion

4.3.2.1. The aggregation of the lipidoids

From **Figure 30** and **Figure 32**, it is clear that the lipidoids can aggregate together in the buffer solution. However, the micelle structure were not formed in both of these two models, which is different with the expected output. Considering the size the lipidoids, we believe that the reason why lipidoids don't form micelles is that the simulation system is too small for forming a micelle. To be specific, the usual length of the lipidoid is around 28 A, while the simulation model is a water box whose size is $80 \times 80 \times 80$ A, which is relatively too small for a micelle considering the length of the lipidoids. The

improvement of the simulation in this part will be discussed in the future direction section.

4.3.2.2. The stability of the bilayer structure

4.3.2.2.1. The implicit solvent model

Though the bilayer structure was disrupted in the simulation of the implicit solvent model, there are still some important information indicated in the output.

Here, in order to indicate the stability of the bilayer, the RMSD for the central nitrogen atom in the head group was calculated (See **Figure 38**), which can be used to indicate the stability of the head group of the lipidoids in the simulation.

(a)

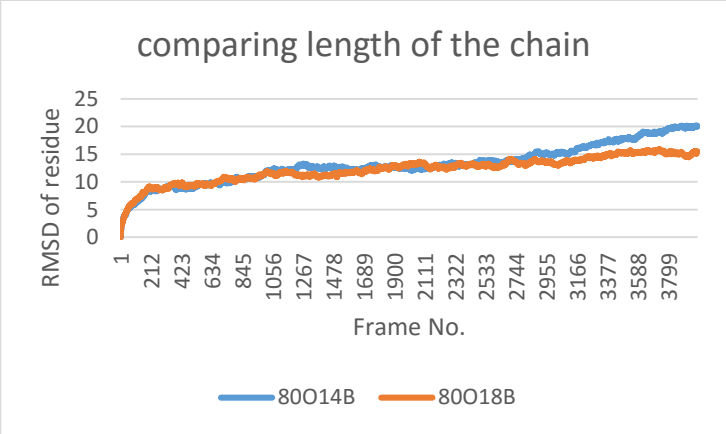

(b)

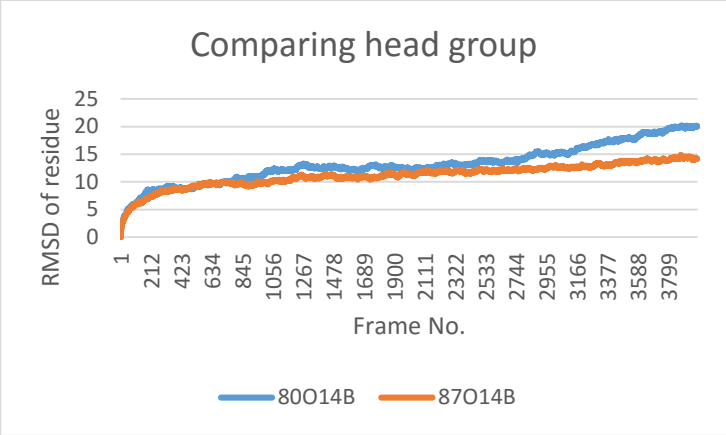

(c)

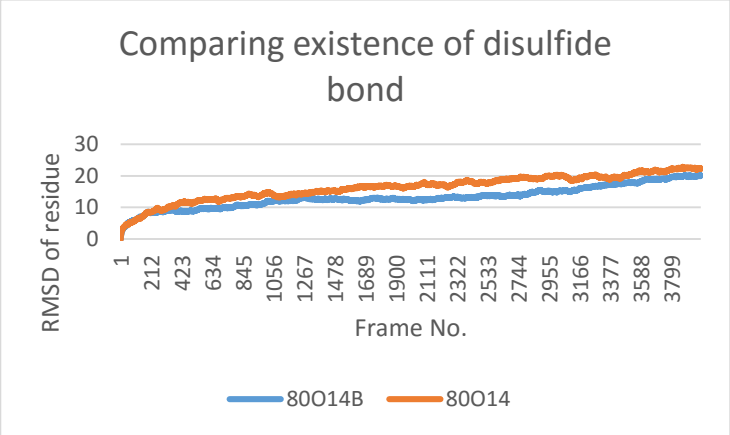

Figure 38 The comparison between the RMSD of the central nitrogen atom of the head group
(a) comparing lipidoids with different length of alkyl chains (b) comparing lipidoids with different head groups (c) comparing lipidoids with disulfide bond and lipidoids without disulfide bond

By looking at this figure, some conclusions have been found:

First, with the increase of the length of the alkyl chain, the head group will be more stable.

Second, the “87” head group has better stability comparing to the “80” head group.

Third, the lipidoids with disulfide bond has the more stable head group.

4.3.2.2.2. The explicit solvent model

Since the explicit solvent model includes the real water molecules and ions in the system, it is typically more accurate compared to the implicit solvent model. Thus, though the results of these two models are different, we believe that the explicit solvent model has a more convincing result. In other words, the bilayer structure can maintain stability within the buffer solution.

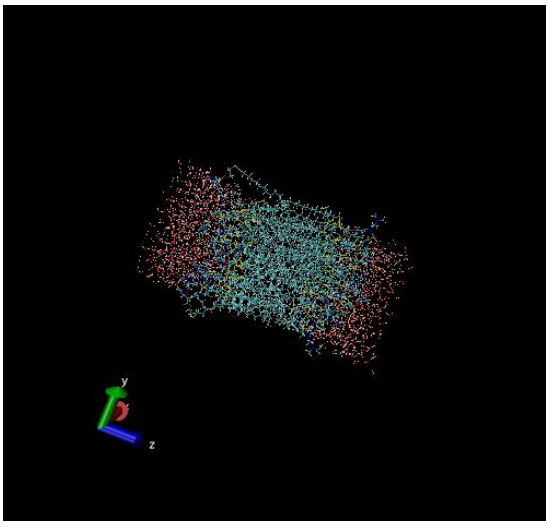

(a) 80O18B

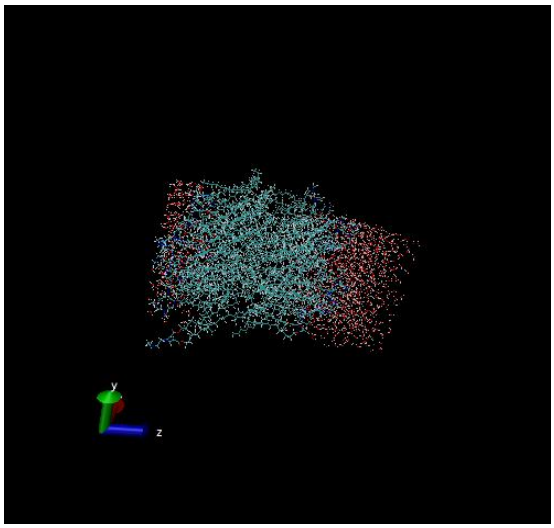

(b) 80O18

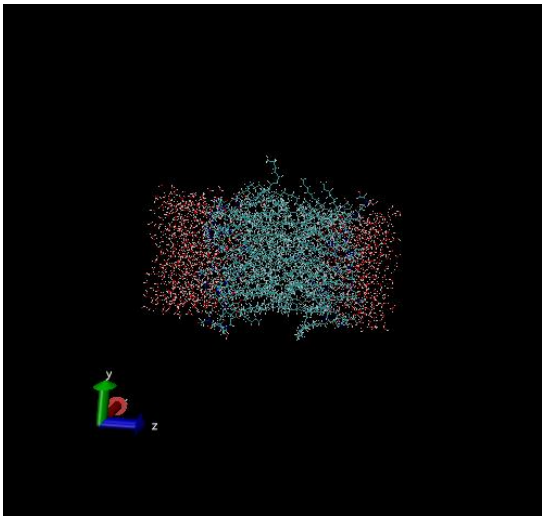

(c) 87O14

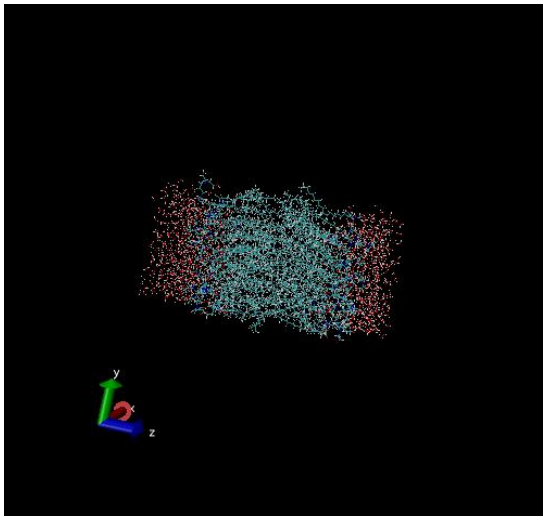

(d) 87O18

Figure 39 The final state of the bilayer of different lipidoids in the explicit solvent model (a) 80O18B (b) 80O18 (c) 87O14 (d) 87O18

Figure 39 includes the final state of four different lipidoids. Through observing these four final states, it was visible that the stability of 80O18 was the worst, while the other 3 lipidoids could form more stable bilayers.

Considering that 80O18 has no disulfide bond and “87” head group, it is concluded that the CMC value of 80O18 will be relatively higher, which indicates that the 80O18 does not form micelles with relative ease. In addition, the 1:3 ratio of 80O18 when pyrene in the micelle is also higher than that of other lipidoids. This represents the polarity of inner space of the micelle formed by 80O18 is higher than that of other lipidoids.

Through analysis of the simulation result, we believe that the lipidoids with lower CMC value and 1:3 ratio can form a more stable bilayer structure. In other words, for the lipidoids which can form micelles easily, their bilayer structure will be relatively more stable as well.

Chapter 5 Conclusions and Future Direction

5.1. Summary

The goal of this thesis is to study the relationship between the molecular structure and the micellization property of the lipidoids. Future research will continue to focus on the investigation of the physical property like the morphology of the micelles, and the fluorescent quenching property. Molecular Dynamic (MD) simulation will be conducted in a larger system as well.

In the 1:3 ratio method for measuring the CMC value of different molecules, we completed the preliminary experiment with SDS and calculated its CMC value. Through comparison with the data of SDS from the reference[24], we proved that the 1:3 ratio method was feasible for measuring the CMC value for surfactants. Then, considering that the sonication of the sample solution with lipidoid may involve a dynamic change on the physical property of the solution, we measured the emission spectra with the increase of time and compared the emission spectrum and the 1:3 ratio at different times when the concentration was the same. It was found that the effects of the time was significant on the intensity of the emission spectrum but very insignificant on the 1:3 ratio. This conclusions indicated that the effects of time on the 1:3 ratio method could be ignored. Then, the 1:3 ratio of different lipidoids at different concentration was measured and used for calculation of the CMC value for the corresponding lipidoid. Through the experiment,

we confirmed that the structure of the lipidoid including the length of the alkyl chain, the head group and the disulfide bond could affect the tendency of the self-assembly of lipidoids significantly. Besides that, the polarity of the inner space of the micelle which is profiled by 1:3 ratio has negative correlation with the tendency of self-assembly. In addition, considering the changing pattern of the intensity of the emission spectrum with the increase of the concentration of lipidoids, we hypothesized that the lipidoids had the fluorescence quenching capability.

In the AFM image of sample solution of the lipidoids at high concentration, multiple micelles with spherical shape were observed and the radius were around 60 nm ~ 80 nm. This result provided the direct proof for the micellization of the lipidoids at the concentration which was higher than CMC value.

In the simulation of the lipidoids through different models. The aggregation of the lipidoids at high concentration was proved. However, since the scale of the simulation system was too small to form micelles during the simulation, the typical structure of micelle was not found. In the explicit solvent model for checking the stability of the bilayer structure, through the analysis of RMSD data, total energy and the temperature fluctuation, it was concluded that the bilayer structure could be stable at the equilibrium state of the system. Through observing the behavior of the lipidoids in the bilayer, it was found that the bilayer formed by lipidoids with high CMC value were relatively unstable

comparing to other bilayer structure, which supported our previous conclusions in another way.

Through this thesis, the relationship between the property of the micellization and the structure of the lipid-like molecules was confirmed. The head group, disulfide bond, and the length of the alkyl china could affect the tendency of self-assembly and the stability of the bilayer significantly. When the concentration of the lipid-like molecules was higher than the CMC value we calculated, the sphere micelles could be found through AFM instrument. In addition, we also proposed that the lipid-like molecules had the fluorescence quenching capability.

5.2. Future Direction

According to the previous research and conclusions, the future work could focus on several areas.

We will calculate the CMC value of more lipid-like through 1:3 ratio methods and investigate the relationship between the CMC value and the structure of the molecules. For example, in the lipid-like molecules, the number of the alkyl chain can be one, two, or three and the lipid-like molecules with three alkyl chains has been synthesized. The CMC value of these lipidoids may be different with the lipidoids with two alkyl chains.

The AFM will be utilized for taking the images of more different lipid-like molecules at the concentration higher than CMC value. The relationship between the morphology of the micelles and the structure of the lipidoids will also be investigated.

The scale of the simulation system will be enlarged to more than $100 \times 100 \times 100$ A so that the lipidoids could form micelles within the simulation system. In addition, we will also utilize the software Packmol to construct the micelle structure and the liposome structure with the explicit water molecules and ions and check the stability of these structures by simulation.

Reference

[1] Freitas, Robert A. *Nanomedicine, volume I: basic capabilities*. Georgetown, TX: Landes Bioscience, 1999.

[2] Moghimi, S. Moein, A. Christy Hunter, and J. Clifford Murray. "Nanomedicine: current status and future prospects." *The FASEB Journal* 19.3 (2005): 311-330.

[3] Freitas, Robert A. "What is nanomedicine?."*Nanomedicine: Nanotechnology, Biology and Medicine* 1.1 (2005): 2-9.

[4] Allen, Theresa M., and Pieter R. Cullis. "Drug delivery systems: entering the mainstream."*Science* 303.5665 (2004): 1818-1822.

[5] Kalepu, Sandeep, Mohanvarma Manthina, and Veerabhadhraswamy Padavala. "Oral lipid-based drug delivery systems–an overview." *Acta Pharmaceutica Sinica B* 3.6 (2013): 361-372.

[6] Shrestha, Hina, Rajni Bala, and Sandeep Arora. "Lipid-based drug delivery systems." *Journal of Pharmaceutics* 2014 (2014).

[7] Prabhu, Sunil, Maru Ortega, and Chan Ma. "Novel lipid-based formulations enhancing the in vitro dissolution and permeability characteristics of a poorly water-soluble model drug, piroxicam."*International journal of pharmaceutics* 301.1 (2005): 209-216.

[8] Kazunori, Kataoka, et al. "Block copolymer micelles as vehicles for drug delivery." *Journal of Controlled Release* 24.1 (1993): 119-132.

[9] Liechty, William B., et al. "Polymers for drug delivery systems." *Annual review of chemical and biomolecular engineering* 1 (2010): 149.

[10] Ojea-Jimenez, Isaac, et al. "Engineered inorganic nanoparticles for drug delivery applications."*Current drug metabolism* 14.5 (2013): 518-530.

[11] Liong, Monty, et al. "Multifunctional inorganic nanoparticles for imaging, targeting, and drug delivery." *ACS nano* 2.5 (2008): 889-896.

[12] Akinc, Akin, et al. "A combinatorial library of lipid-like materials for delivery of RNAi therapeutics."*Nature biotechnology* 26.5 (2008): 561-569.

[13] Whitehead, Kathryn A., et al. "Degradable lipid nanoparticles with predictable in vivo siRNA delivery activity." *Nature communications* 5 (2014).

[14] Wang, Ming, et al. "Enhanced Intracellular siRNA Delivery using Bioreducible Lipid-Like Nanoparticles." *Advanced healthcare materials* 3.9 (2014): 1398-1403.

[15] Sun, Shuo, et al. "Combinatorial library of lipidoids for in vitro DNA delivery." *Bioconjugate chemistry*23.1 (2011): 135-140.

[16] Wang, Ming, et al. "A combinatorial library of unsaturated lipidoids for efficient intracellular gene delivery." *ACS synthetic biology* 1.9 (2012): 403-407.

[17] Wang, Ming, et al. "Combinatorially Designed Lipid-like Nanoparticles for Intracellular Delivery of Cytotoxic Protein for Cancer Therapy."*Angewandte Chemie* 126.11 (2014): 2937-2942.

[18] Wang, Ming, and Qiaobing Xu. "Combinatorial cationic lipid-like nanoparticles for efficient intracellular cytotoxic protein delivery." *Northeast Bioengineering Conference (NEBEC), 2014 40th Annual*. IEEE, 2014.

[19] De Aguiar, Hilton B., et al. "Surface structure of sodium dodecyl sulfate surfactant and oil at the oil-in-water droplet liquid/liquid interface: a manifestation of a nonequilibrium surface state." *The Journal of Physical Chemistry B* 115.12 (2011): 2970-2978.

[20] Wilhelm, Manfred et al. "Poly (styrene-ethylene oxide) block copolymer micelle formation in water: a fluorescence probe study." Macromolecules 24.5 (1991): 1033-1040.

[21] Kalyanasundaram, K., and J. K. Thomas. "Environmental effects on vibronic band intensities in pyrene monomer fluorescence and their application in studies of micellar systems."*Journal of the American Chemical Society* 99.7 (1977): 2039-2044.

[22] Dong, Bin, et al. "Aggregation behavior of long-chain imidazolium ionic liquids in aqueous solution: micellization and characterization of micelle microenvironment." *Colloids and Surfaces A: Physicochemical and Engineering Aspects*317.1 (2008): 666-672.

[23] Dominguez, Ana et al. "Determination of critical micelle concentration of some surfactants by three techniques." *Journal of Chemical Education* 74.10 (1997): 1227.

[24] Aguiar, J et al. "On the determination of the critical micelle concentration by the pyrene 1: 3 ratio method." *Journal of Colloid and Interface Science* 258.1 (2003): 116-122.

[25] Chen, Yongzhu, et al. "Self-assembling surfactant-like peptide A6K as potential delivery system for hydrophobic drugs." *International journal of nanomedicine* 10 (2015): 847.

[26] Dong, Xuemeng, and Chenguang Liu. "Preparation and characterization of self-assembled nanoparticles of hyaluronic acid-deoxycholic acid conjugates." *Journal of Nanomaterials* 2010 (2010): 12.

[27] Giessibl, Franz J. "Advances in atomic force microscopy." *Reviews of modern physics* 75.3 (2003): 949.

[28] Binnig, Gerd, Calvin F. Quate, and Ch Gerber. "Atomic force microscope." *Physical review letters* 56.9 (1986): 930.

[29] Bennig, Gerd K. "Atomic force microscope and method for imaging surfaces with atomic resolution." U.S. Patent No. 4,724,318. 9 Feb. 1988.

[30] The Common AFM Modes (1997). Retrieved from http://www.chembio.uoguelph.ca/educmat/chm729/afm/details.htm

[31] Zhong, Q., et al. "Fractured polymer/silica fiber surface studied by tapping mode atomic force microscopy." *Surface Science Letters* 290.1 (1993): L688-L692.

[32] Geisse, Nicholas A. "AFM and combined optical techniques." *Materials today* 12.7 (2009): 40-45.

[33] Ray, Gargi Basu, Indranil Chakraborty, and Satya P. Moulik. "Pyrene absorption can be a convenient method for probing critical micellar concentration (cmc) and indexing micellar polarity." *Journal of colloid and interface science*294.1 (2006): 248-254.

[34] Dong, Bin, et al. "Aggregation behavior of long-chain imidazolium ionic liquids in aqueous solution: micellization and characterization of micelle microenvironment." *Colloids and Surfaces A: Physicochemical and Engineering Aspects*317.1 (2008): 666-672.

[35] Wilhelm, Manfred, et al. "Poly (styrene-ethylene oxide) block copolymer micelle formation in water: a fluorescence probe study." *Macromolecules*24.5 (1991): 1033-1040.

[36] Turro, Nicholas J., and Ahmad Yekta. "Luminescent probes for detergent solutions. A simple procedure for determination of the mean aggregation number of micelles." *Journal of the American Chemical Society* 100.18 (1978): 5951-5952.

[37] Cavalieri, Francesca, Ester Chiessi, and Gaio Paradossi. "Chaperone-like activity of nanoparticles of hydrophobized poly (vinyl alcohol)." *Soft Matter* 3.6 (2007): 718-724.

[38] Dong, Bin, et al. "Aggregation behavior of long-chain imidazolium ionic liquids in aqueous solution: micellization and characterization of micelle microenvironment." *Colloids and Surfaces A: Physicochemical and Engineering Aspects*317.1 (2008): 666-672.

[39] Liaw, Jiahorng, et al. "Visualization of PEO-PBLA-pyrene polymeric micelles by atomic force microscopy." *Pharmaceutical research* 15.11 (1998): 1721-1726.

[40] Ouanezar, Mustapha, Fanny Guyomarc'h, and Antoine Bouchoux. "AFM imaging of milk casein micelles: evidence for structural rearrangement upon acidification." *Langmuir* 28.11 (2012): 4915-4919.

[41] Frenkel, Daan, and Berend Smit. *Understanding molecular simulation: from algorithms to applications*. Vol. 1. Academic press, 2001.

[42] Allen, Michael P. "Introduction to molecular dynamics simulation." *Computational Soft Matter: From Synthetic Polymers to Proteins* 23 (2004): 1-28.

[43] Nelson, Mark T., et al. "NAMD: a parallel, object-oriented molecular dynamics program."*International Journal of High Performance Computing Applications* 10.4 (1996): 251-268.

[44] Villa, Elizabeth, Alexander Balaeff, and Klaus Schulten. "Structural dynamics of the lac repressor–DNA complex revealed by a multiscale simulation." *Proceedings of the National Academy of Sciences of the United States of America*102.19 (2005): 6783-6788.

[45] Humphrey, William, Andrew Dalke, and Klaus Schulten. "VMD: visual molecular dynamics."*Journal of molecular graphics* 14.1 (1996): 33-38.

[46] Phillips, James C., et al. "Scalable molecular dynamics with NAMD." *Journal of computational chemistry* 26.16 (2005): 1781-1802.

[47] L. Mart ńez, R. Andrade, E. G. Birgin, J. M. Mart ńez. Packmol: A package for building initial configurations for molecular dynamics simulations. *Journal of Computational Chemistry*, 30(13):2157-2164, 2009.

[48] Bhandarkar, M., et al. "NAMD User's Guide."*Urbana* 51 (2003): 61801.

[49] Phillips, J., et al. "Namd tutorial." *Accessed in June* (2013).

[50] Bernstein, Frances C., et al. "The Protein Data Bank: a computer-based archival file for macromolecular structures." *Archives of biochemistry and biophysics* 185.2 (1978): 584-591.

[51] Berman, Helen M., et al. "The protein data bank."*Nucleic acids research* 28.1 (2000): 235-242.

[52] MacKerell, Alexander D., Nilesh Banavali, and Nicolas Foloppe. "Development and current status of the CHARMM force field for nucleic acids."*Biopolymers* 56.4 (2000): 257-265.